TEXTE
41/2011

Erfassung, Prognose und Bewertung von Stoffeinträgen und ihren Wirkungen in Deutschland

Anhänge 6 bis 10

Umwelt Bundes Amt
Für Mensch und Umwelt

| TEXTE | 41/2011

UMWELTFORSCHUNGSPLAN DES
BUNDESMINISTERIUMS FÜR UMWELT,
NATURSCHUTZ UND REAKTORSICHERHEIT

Forschungskennzahl 3707 64 200
UBA-FB 001490/ANH, 1

Erfassung, Prognose und Bewertung von Stoffeinträgen und ihren Wirkungen in Deutschland

Anhänge 6 bis 10

von

Prof. Dr. Peter Builtjes
Elise Hendriks
Marielle Koenen
Dr. Martijn Schaap
TNO, Utrecht (Niederlande)

Sabine Banzhaf
Dr. Andreas Kerschbaumer
FU-Berlin, Berlin

Thomas Gauger
INS-Stuttgart, Stuttgart

Dr. Hans-Dieter Nagel
Thomas Scheuschner
Dr. Angela Schlutow
ÖKO-DATA, Strausberg

Im Auftrag des Umweltbundesamtes

UMWELTBUNDESAMT

Diese Publikation ist ausschließlich als Download unter
http://www.uba.de/uba-info-medien/4140.html verfügbar.
Hier finden Sie den Hauptbericht und weitere Anhänge.

Die in der Studie geäußerten Ansichten
und Meinungen müssen nicht mit denen des
Herausgebers übereinstimmen.

ISSN 1862-4804

Durchführung der Studie: TNO, Niederlande
P.O. Box 80015
3508 TA Utrecht (The Netherlands)

Abschlussdatum: Juni 2009

Herausgeber: Umweltbundesamt
Wörlitzer Platz 1
06844 Dessau-Roßlau
Tel.: 0340/2103-0
Telefax: 0340/2103-0
E-Mail: info@umweltbundesamt.de
Internet: http://www.umweltbundesamt.de
http://fuer-mensch-und-umwelt.de/

Redaktion: Fachgebiet II 4.3 Wirkungen von Luftverunreinigungen auf terrestrische Ökosysteme

Markus Geupel, Jakob Frommer

Dessau-Roßlau, Juli 2011

Detailed modeling of dry deposition over Germany

A. **Kerschbaumer, T. Gauger, E. Hendriks, P. Builjtes**

Institut für Meteorologie, FU-Berlin, Germany. Institut für Navigation, Universität Stuttgart, Germany. TNO, The Netherlands.

Abstract

The chemistry transport models REM_Calgrid and LOTOS-EUROS have been used to simulate annual total deposition fluxes on German ecosystems for the whole year 2005. To evaluate these results only indirect measurements are available, i.e. wind turbulence, air pollution concentrations and deduced deposition fluxes over specific ecosystems. The comparison of friction velocities processed from COSMO_EU and from ECMWF has shown good agreement with measurements with correlation coefficients around 0.8. Nitrogen deposition fluxes calculated with the two models for the year 2005 were comparable giving the same spatial distribution and summed over the whole area similar amounts. Comparisons with measured values at a forest site in Augustendorf for the year 2003 have shown substantial differences between the two models, both underestimating the measured nitrogen deposition flux.

Introduction

Deposited loads of sulfur and nitrogen compounds, stemming from anthropogenic precursors, endanger ecosystems and need to be modeled in order to assess the effectiveness of action plans. Model results have shown that approximately 40% of total pollutants deposition is due to wet processes and 60% to dry deposition. At the same time dry deposition is very difficult to measure as it depends on atmospheric stability and on individual receptors of specific pollutants, altogether. The absorbed species concentration in the stomata of different plants, for example, is almost impossible to measure, or to generalize for bigger areas. Measurements are thus a combination of observed air concentrations and micrometeorological measurements and modeled absorption processes for individual ecosystems (Dämmgen, 2005). The same model approach for dry deposition processes is implemented in Chemistry-Transport-Models. The process itself determines, next to emission loads, transport and air chemistry, the quality of air pollution concentration simu-

lations. A thorough model evaluation needs thus to account for dry deposition fluxes and their intrinsic parameters, i.e. atmospheric stability, land classification and air pollution concentration gradients. We performed a model evaluation with respect to dry deposition fluxes comparing independent meteorological measurements and total nitrogen fluxes to a forest site in Germany for two Eulerian Chemistry Transport Models for different time periods.

Methods

The off-line chemistry transport models (CTM) REM_Calgrid (RCG) (Stern et al., 2003) and LOTOS-EUROS (LE) (Schaap et al., 2008) simulate air pollution concentrations and deposition solving the advection-diffusion equation with a horizontal resolution of approximately 7x7 km² and up to 3500 m height. Emissions for Germany were delivered from local and national inventories, while European emissions are based on EMEP data post-processed at TNO (Klotz et al., 2009). Meteorological fields were taken from COSMO-EU (DWD) for RCG and from ECMWF for LE. Both CTM were evaluated within the framework of several European model inter-comparison studies (e.g. Cuvelier et al., 2007).

Dry deposition velocity is parameterised in both CTM following the resistance approach proposed by Erisman et al. (1994). The atmospheric resistance R_a and the sublayer resistance R_b are driven by the friction velocity u_* and the atmospheric stability Ψ_m. which is parameterised with the Monin-Obukhov-Length (L). The canopy resistance for gases depends largely on the surface humidity and on plant physiological parameters. Friction velocity u_* is one of the most prominent parameters in simulating dry deposition processes. At Lindenberg in the South-East of Berlin, DWD has been performing turbulence measurements since more than 10 years. A 28 m measurement tower at the forest site was equipped with meteorological measurement devices at different levels with sampling times for temperature, humidity, wind speed and direction of one second. (Beyrich et al., 2007). Turbulent momentum fluxes were determined from the high resolution measurements of the three wind components by computing mean eddy covariances and used to compute the friction velocity. The nitrogen deposition measurements at the forest site in Augustendorf in the North-Western plain land of Germany, have been derived using the micrometeorological method described in Dämmgen (2005) which uses the eddy covariance assumption coded in the PLATIN-model (Grünhage et al., 2008). The model calculates the exchange of trace gases and fine-particle constituents. The vertical transport between an above-canopy reference height, for which air properties and concentrations of matter must be known, and the sinks and/or sources of the plant/soil-surface system is estimated. The air pollution concentrations were measured using in series denuder tubes (Dämmgen, 2005) for gaseous NH_3, HNO_2, HNO_3, SO_2 and HCL and for particles NH_4-N, NO_3-N, SO_4-S, Cl and Na. Wind speed and direction, air temperature and humid-

ity were measured at 25 m as well as at 22 m above ground, with an average sampling period of 15 minutes.

Results and Discussion

Figure 1 shows the hourly performance of the friction velocity simulations (y-axis) compared to the forest measurement sites in Lindenberg (x-axis), derived for RCG from the dynamic model COSMO-EU (left panel) and for LE from the ECMWF-model (right panel). Taking into account that both meteorological models comprise more than one land-use-type in one cell, friction velocities are well reproduced temporally with correlation coefficients around 0.8 for both models slightly underestimating measurements (slope 0.6 and intercept 0.13 m/s for COSMO_EU and 0.76 slope and intercept 0.16 m/s for ECMWF).

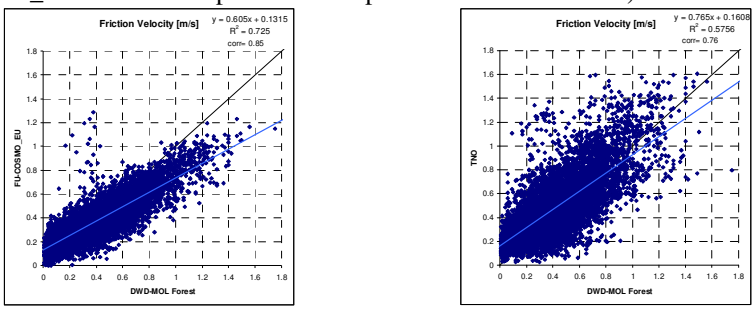

Fig. 1. Model (y-axis) friction velocity compared to measurements (x-axis) for COSMO_EU (left) and ECMWF (right).

Figure 2 shows the total nitrogen deposition fluxes simulated with the two CTM for the year 2005. The spatial distribution is very similar in both models emphasizing areas with high NOx – emissions in Germany. Also the absolute values are comparable. For the year 2003 measurements from Augustendorf were available and have been used to validate RCG and LE for this year at this forest-site. Table 1 gives the accumulated observed and simulated gaseous and solid nitrogen fluxes. RCG simulates very well NH_3 on a yearly basis while LE overestimates ammonia. Both models underestimate heavily aerosol ammonia and aerosol nitrate, while NO_2 is again reproduced correctly. The total nitrogen deposition at the observation site in the forest is depicted well with LE (ca. 20% less) and underestimated by 60% with RCG. The good performance of LE is partially due to the overestimation of NH_3. A point to grid comparison is difficult and not always representative, nevertheless available micrometeorological observations and measured deposition fluxes are at the same order of magnitude as modeled values.

Acknowledgments This work has been funded by Umweltbundesamt - Germany within the R&D-project MAPESI under Contract No. 3707 64 200.

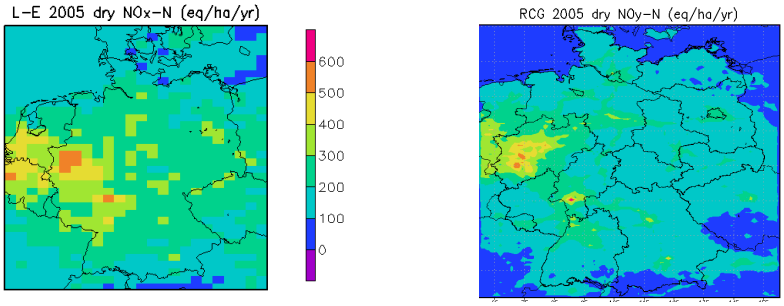

Fig. 2. Total nitrogen deposition flux, accumulated for 2005, simulated with LE (left) and with RCG (right) in eq/ha-a.

Table 1. and simulated accumulated annual deposition fluxes for gaseous and aerosol N-species in Augustendorf – Germany.

species [kg-N/ha-a]	observed	RCG	LE
NH_3	16.2	16.1	26.5
NH_4	14.1	0.1	3.0
NO_3	8.2	0.1	2.0
HNO_3	2.9	0.6	0.9
NO_2	1.5	1.9	1.7
HNO_2	0.8	0.0	0.0
TOTAL	43.7	18.6	34.1

References

Beyrich, F. and W. K. Adam (2007). Site and Data Report for the Lindenberg Reference Site in CEOP – Phase I. Berichte des Deutschen Wetterdienstes, 230. Selbstverlag des Deutschen Wetterdienstes, 55 pp.

Cuvelier, C. et al., (2007). CityDelta: A model intercomparison study to explore the impact of emission reductions in European cities in 2010, Atmos. Env., 41, 189-207.

Dämmgen, U. (Ed.) (2005). Bestimmung von Ammoniak-Einträgen aus der Luft und deren Wirkung auf Waldökosysteme (ANWER-Projekt). Landbauforschung Völkenrode, Special Issue 279, 128 pp.

Erisman, J.W., A. van Pul and P. Wyers (1994). Parametrization of surface-resistance for the quantification of atmospheric deposition of acidifying pollutants and ozone, Atmos. Environ., **28**, 2595-2607.

Grünhage, L., and H.-D. Haenel (2008). PLATIN - PLant-ATmosphere INteraction model. Landbauforschung Völkenrode, Special Issue 319, 85 pp.

Klotz, V., et al. (2009). An integrated measure-based approach to fulfil European air quality targets cost-effective on a national level - First results of the German PAREST-project. TFIAM Meeting, 10. Juni, Bilthoven, Niederlande

Schaap M., F. Sauter, R.M.A. Timmermans, M. Roemer, G. Velders, J. Beck and P.J.H. Builtjes (2008). The LOTOS–EUROS model: description, validation and the latest developments, *Int. J. Environ. Pollut.* **32** (2), pp. 270–290.

Stern, R., Yamartino, R., Graff, A. (2003). Dispersion Modelling within the European Community's air quality directives: Long term modelling of O_3, PM10 and NO_2. 26th ITM, Turkey.

Modellierung der N-Deposition mit und ohne NH_3-Emissionen einzelner Landkreise
Landkreis Coesfeld
Mittlere NH_3-N Emissionen (LUA-Homepage Luft 2006: 7801 t/a NH_3): 58 kg ha^{-1} a^{-1} NH_3-N
„Normale“ Modellierung – Kartenstatistik Coesfeld:
Mittlere NH_X-N Gesamtdeposition 2005: 25 kg ha^{-1} a^{-1}
Mittlere NO_Y-N Gesamtdeposition 2005: 9 kg ha^{-1} a^{-1}
Mittlere N Gesamtdeposition 2005: 34 kg ha^{-1} a^{-1}
Mittlere NH_X-N Nassdeposition 2005: 7 kg ha^{-1} a^{-1}
Mittlere NO_Y-N Nassdeposition 2005: 4 kg ha^{-1} a^{-1}
Mittlere N Nassdeposition 2005: 11 kg ha^{-1} a^{-1}
Mittlere NH_X-N Trockendeposition 2005: 19 kg ha^{-1} a^{-1}
Mittlere NO_Y-N Trockendeposition 2005: 5 kg ha^{-1} a^{-1}
Mittlere N Trockendeposition 2005: 23 kg ha^{-1} a^{-1}
Modellierung ohne NH_3-Emissionen in COE – Kartenstatistik Coesfeld*:
[* ohne Berücksichtigung der Minderung in der Nassdeposition]
Mittlere NH_X-N Gesamtdeposition 2005: 16 kg ha^{-1} a^{-1} (ca. -9,7; -40% auf 60%)*
Mittlere NO_Y-N Gesamtdeposition 2005: 9 kg ha^{-1} a^{-1}
Mittlere N Gesamtdeposition 2005: 24 kg ha^{-1} a^{-1} (ca. -9,5; -29% auf 71%)*
Mittlere NH_X-N Nassdeposition 2005: 7 kg ha^{-1} a^{-1}
Mittlere NO_Y-N Nassdeposition 2005: 4 kg ha^{-1} a^{-1}
Mittlere N Nassdeposition 2005: 11 kg ha^{-1} a^{-1}
Mittlere NH_X-N Trockendeposition 2005: 9 kg ha^{-1} a^{-1} (ca. -9,7; -54%, auf 46%)
Mittlere NO_Y-N Trockendeposition 2005: 5 kg ha^{-1} a^{-1}
Mittlere N Trockendeposition 2005: 14 kg ha^{-1} a^{-1}
Durch Rundungen sind die Berechnungen/Angaben der Kartenstatistik nicht immer ganz ausgeglichen!

Ergebnisse und kurze Interpretation:
- Die Größenordnung der NH_3-Netto-Emissionen im LKR COE ist deutlich höher als die NH_X-N Gesamtdeposition (COE exportiert nach dieser Netto-Bilanz grob die Hälfte der Emissionen)
- Das „Ausblenden“ der NH_3-Emissionen ergibt eine deutliche Minderung der NH_X-N Trockendeposition um 54%, d.h. rechnerisch werden 46% der NH_X-N Trockendeposition nach COE importiert.
- Die Minderung in der Nassdeposition ist hier nicht berücksichtigt!
- Die NH_X-N-Gesamtdeposition (trockene + nasse Deposition) vermindert sich so um 40%.
- Insgesamt 60% der NH_X-N-Gesamtdeposition im LKR Coesfeld werden demnach importiert.
- Die N-Gesamtdeposition vermindert sich nach dieser Berechnung um 29%
- Für eine ausgeglichene Massenbilanz wäre für den Landkreis somit die NH_3-N Gesamtdeposition von knapp 10 kg ha^{-1} a^{-1} , bzw. im Landkreis COE insgesamt ca. 1077 t/a NH_3-N (ca. 29% der N-Gesamtdeposition) mit einer Berechnung durch AUSTAL zu ersetzen

Modellierung der N-Deposition mit und ohne NH_3-Emissionen einzelner Landkreise
Landkreis Traunstein
Mittlere NH_3-N Emissionen (Emissionskataster Bayern, 2000): 3148 t/a NH_3) : 18 kg ha^{-1} a^{-1} NH_3-N
„Normale“ Modellierung – Kartenstatistik Traunstein:
Mittlere NH_X-N Gesamtdeposition 2005: 17 kg ha^{-1} a^{-1}
Mittlere NO_Y-N Gesamtdeposition 2005: 8 kg ha^{-1} a^{-1}
Mittlere N Gesamtdeposition 2005: 25 kg ha^{-1} a^{-1}
Mittlere NH_X-N Nassdeposition 2005: 8 kg ha^{-1} a^{-1}
Mittlere NO_Y-N Nassdeposition 2005: 5 kg ha^{-1} a^{-1}
Mittlere N Nassdeposition 2005: 13 kg ha^{-1} a^{-1}
Mittlere NH_X-N Trockendeposition 2005: 9 kg ha^{-1} a^{-1}
Mittlere NO_Y-N Trockendeposition 2005: 2 kg ha^{-1} a^{-1}
Mittlere N Trockendeposition 2005: 11 kg ha^{-1} a^{-1}

Modellierung ohne NH_3-Emissionen in TS – Kartenstatistik Traunstein*:
[* ohne Berücksichtigung der Minderung in der Nassdeposition]
Mittlere NH_X-N Gesamtdeposition 2005: 11 kg ha^{-1} a^{-1} (ca. -5,2; -31% auf 69%)*
Mittlere NO_Y-N Gesamtdeposition 2005: 8 kg ha^{-1} a^{-1}
Mittlere N Gesamtdeposition 2005: 19 kg ha^{-1} a^{-1} (ca. -5,7; -21% auf 79%)*
Mittlere NH_X-N Nassdeposition 2005: 8 kg ha^{-1} a^{-1}
Mittlere NO_Y-N Nassdeposition 2005: 5 kg ha^{-1} a^{-1}
Mittlere N Nassdeposition 2005: 13 kg ha^{-1} a^{-1}
Mittlere NH_X-N Trockendeposition 2005: 3 kg ha^{-1} a^{-1} (ca. -5,2; -60%, auf 40%)
Mittlere NO_Y-N Trockendeposition 2005: 3 kg ha^{-1} a^{-1}
Mittlere N Trockendeposition 2005: 6 kg ha^{-1} a^{-1}
Durch Rundungen sind die Berechnungen/Angaben der Kartenstatistik nicht immer ganz ausgeglichen!

Ergebnisse und kurze Interpretation:
- Die Größenordnung der NH_3-Netto-Emissionen im LKR TS ist fast gleich groß wie die NH_X-N Gesamtdeposition (TS hat eine in etwa ausgeglichene Netto-Bilanz)
- Das „Ausblenden“ der NH_3-Emissionen ergibt eine deutliche Minderung der NH_X-N Trockendeposition um 60%, d.h. rechnerisch werden 40% der NH_X-N Trockendeposition nach TS importiert.
- Die Minderung in der Nassdeposition ist hier nicht berücksichtigt!
- Die NH_X-N-Gesamtdeposition (trockene + nasse Deposition) vermindert sich so um 31%.
- Insgesamt 69% der NH_X-N-Gesamtdeposition im LKR Traunstein werden demnach importiert.
- Die N-Gesamtdeposition vermindert sich nach dieser Berechnung um 21%
- Für eine ausgeglichene Massenbilanz wäre für den Landkreis somit die NH_3-N Gesamtdeposition von ca. 5 kg ha^{-1} a^{-1}, bzw. im Landkreis UM insgesamt ca. 734 t/a NH_3-N (ca. 21% der N-Gesamtdeposition) mit einer Berechnung durch AUSTAL zu ersetzen

Modellierung der N-Deposition mit und ohne NH_3-Emissionen einzelner Landkreise
Landkreis Uckermark
Mittlere NH_3-N Emissionen (FAL, nur landwi. Emissionen, 2003: 2571 t/a NH_3): 7 kg ha^{-1} a^{-1} NH_3-N
„Normale“ Modellierung – Kartenstatistik Uckermark:
Mittlere NH_X-N Gesamtdeposition 2005: 8 kg ha^{-1} a^{-1}
Mittlere NO_Y-N Gesamtdeposition 2005: 5 kg ha^{-1} a^{-1}
Mittlere N Gesamtdeposition 2005: 13 kg ha^{-1} a^{-1}
Mittlere NH_X-N Nassdeposition 2005: 4 kg ha^{-1} a^{-1}
Mittlere NO_Y-N Nassdeposition 2005: 2 kg ha^{-1} a^{-1}
Mittlere N Nassdeposition 2005: 6 kg ha^{-1} a^{-1}
Mittlere NH_X-N Trockendeposition 2005: 4 kg ha^{-1} a^{-1}
Mittlere NO_Y-N Trockendeposition 2005: 3 kg ha^{-1} a^{-1}
Mittlere N Trockendeposition 2005: 7 kg ha^{-1} a^{-1}
Modellierung ohne NH_3-Emissionen in UM – Kartenstatistik Uckermark*:
[* ohne Berücksichtigung der Minderung in der Nassdeposition]
Mittlere NH_X-N Gesamtdeposition 2005: 6 kg ha^{-1} a^{-1} (ca. -2,2; -28% auf 72%)*
Mittlere NO_Y-N Gesamtdeposition 2005: 5 kg ha^{-1} a^{-1}
Mittlere N Gesamtdeposition 2005: 11 kg ha^{-1} a^{-1} (ca. -2,0; -15% auf 85%)*
Mittlere NH_X-N Nassdeposition 2005: 4 kg ha^{-1} a^{-1}
Mittlere NO_Y-N Nassdeposition 2005: 2 kg ha^{-1} a^{-1}
Mittlere N Nassdeposition 2005: 6 kg ha^{-1} a^{-1}
Mittlere NH_X-N Trockendeposition 2005: 2 kg ha^{-1} a^{-1} (ca. -2,2; -54%, auf 46%)
Mittlere NO_Y-N Trockendeposition 2005: 3 kg ha^{-1} a^{-1}
Mittlere N Trockendeposition 2005: 5 kg ha^{-1} a^{-1}
Durch Rundungen sind die Berechnungen/Angaben der Kartenstatistik nicht immer ganz ausgeglichen!

Ergebnisse und kurze Interpretation:

- Die Größenordnung der NH_3-Netto-Emissionen im LKR UM ist etwa gleich groß wie NH_X-N Gesamtdeposition (UM hat eine etwa ausgeglichene Netto-Bilanz)
- Das „Ausblenden“ der NH_3-Emissionen ergibt eine deutliche Minderung der NH_X-N Trockendeposition um 54%, d.h. rechnerisch werden 46% der NH_X-N Trockendeposition nach UM importiert.
- Die Minderung in der Nassdeposition ist hier nicht berücksichtigt!
- Die NH_X-N-Gesamtdeposition (trockene + nasse Deposition) vermindert sich so um 28%.
- Insgesamt 72% der NH_X-N-Gesamtdeposition im LKR Uckermark werden demnach importiert.
- Die N-Gesamtdeposition vermindert sich nach dieser Berechnung um 15%
- Für eine ausgeglichene Massenbilanz wäre für den Landkreis somit die NH_3-N Gesamtdeposition von ca. 2 kg ha^{-1} a^{-1} , bzw. im Landkreis UM insgesamt ca. 673 t/a NH_3-N (ca. 15% der N-Gesamtdeposition) mit einer Berechnung durch AUSTAL zu ersetzen

Introduction.

In the framework of MAPESI no modelling of Mercury, Hg, by chemistry transport models, CTM's, has been taken place over Europe and Germany. The question has arisen whether models exists which could be used-in case needed/wanted- to model Mercury.

Mercury (Hg) is a naturally occuring element with a number of unique characteristics, which makes its environmental distribution,and potential for eco-system and human effects, an issue of concern. Mercury is volatile and has an atmospheric lifetime of around a year, making transport on a hemispherical or global scale feasible. Mercury is oxidised in the gas or aqueous phase forming gaseous divalent compounds (usually denoted Reactive Gaseous Mercury, RGM) which are water-soluble and readily deposit to the earth's surface via wet and dry processes. Re-emission of Hg-o from water bodies and land is a significant source and contributes to the long environmental lifetime of Hg. Anthropogenic emissions of Hg are regulated in a number of countries. Mercury is also part of the 1998 Arhus protocol of the UNECE Convention on Long Range Transboundary Air Pollution. (from Munthe and Palm, 2003, also a very good overview of the state-of –the-art till about 2000/2003).
A more recent, comprehensive overview concerning the sources of mercury in deposition can be found in Lindberg et al, 2007.

Modelling of Mercury at a European scale

Several regional chemistry models exists which are capable of modelling mercury.
An intercomparison study has recently been carried out with five regional scale models, with also two hemispheric models and one global model. The study first focussed on the comparison of the algorithms for the pysico-chemical transformations of mercury species in a cloud/fog environment (Ryaboshapko et al, 2002). The second phase of the study had the purpose to compare the models with short-term measurements (Ryaboshapko et al, 2007 a) and the final phase was directed to the comparison of modelling results versus long term observations and the comparison of country deposition budgets (Ryaboshapko 2007 b). The five regional scale models were the ADOM-Model, run by GKSS,Germany, the CMAQ-model run by US-EPA, DEHM, the Danisch model run by NERI, the EMAP-model run by the Inst. of Meteorology and Hydrology in Sofia, Bulgaria and MSCE-HM, run by the Moscow Inst. as part of EMEP.
The set-up of the models is rather similar. The models consider three mercury physico-chemical forms: gaseous elemental mercury (GEM), total particulate mercury (TPM) and reactive gaseous mercury (RGM). The regional models utilize boundary conditions derived from the hemispherical/global models. The emissions for Europe were restricted to anthropogenic emissions, natural emissions and re-emissions were neglected as it was assumed that over Europe the anthropogenic emissions would exert the greatest influence.
The intercomparison concerning the short-term measurements showed significant ability of the five regional scale models to simulate GEM (90% within a factor 1.35) as well as TPM (90 % within a factor 2.5). Largest discrepancies were found for RGM (90 % within a factor 10)
More important for MAPESI is the model performance concerning the long term study. In that study only GEM was considered; the models demonstrated good agreement within +/- 20 %. Modelled values of wet deposition of Hg agreed with observations within +/- 45 %. The scattering of modelling results for dry deposition was for annual averages about +/- 50 %.
The study does not conclude which models would be more appropriate to use. However, it seems that both the ADOM, see also Petersen et al, 2001, and Schmolke and Petersen, 2003, as well as the MSCE-HM model, which is the concensus model used in the framework of EMEP are well suited to model the behaviour of mercury. It should also be mentioned that the CMAQ-model used by the US-EPA, see also Russell Bullock and Brehme, 2002, which also took part in the intercomparison study, is used more and

more in Europe for O3 and PM/Aerosols. Although it seems not to be used in Europe at the moment for mercury, it can be expected that this might happen in the not too distant future..

Observations and Emissions

For some recent studies concerning observations of Mercury at remote sites see Temme et al 2003,and of the Canadian network Temme et al, 2007.
For an evaluation of mercury emissions based on Mace head observation see Slemr et al, 2006, and concerning improved mercury emissions from traffc, see Denier van der Gon et al, 2009

Conclusions

The current anthropogenic Mercury emission data base and modelling capabilities of mercury, make it possible to perform modelling studies of Mercury over Europe with an acceptable accuracy

References

Denier van der Gon, H , Appelman, W. " Lead emissions from road transport in Europe-A revision of current estimates using various estimation methodologies" Science of the total Environment,407, 5367-5372, 2009

Lindberg, S et al. "A Synthesis of Progress and Uncertainties in Attributing the Sources of Mercury in Deposition" Panel on Source Attribution of atmospheric mercury. Ambio 36, 1, 19-32, 2007

Munthe, J. and A. Palm. "The Atmospheric Cycling of Mercury and Persistent Organic Pollutants-MEPOP". EUROTRAC-2 subproject Final Rep.2003

Petersen, G. et al "A comprehensive Eulerian modelling framework for airborne mercury species: model development and applications in Europe". Atm.Env. 35, 3063-3074, 2001

Russell Bullock Jr. O, and K. A. Brehme "Atmospheric mercury simulations using the CMAQ model: formulation and description and analysis of wet deposition results". Atm.Env. 36, 2135-2146, 2002

Ryaboshapko, A, et al " Comparison of mercury chemistry models" Atm. Env. 36, 3881-3898, 2002

Ryaboshapko, A. et al "Intercomparison study of atmospheric mercury models:
1.Comparison of models with short-term measurements". Science of the Total Environment. 376, 228-240, 2007a

Ryaboshapko, A. et al "Intercomparison study of atmospheric mercury models:
2.Modelling results vs. long-term observations and comparison of country deposition budgets". Science of the Total Environment. 376, 319-333, 2007b

Schmolke, S.R. and G.Petersen. "A comprehensive Eulerian modeling framework for airborne mercury species: comparison of model results with data from measurement campaings in Europe'. Atm.Env. 37, Suppl. 1, S51-S62, 2003

Slemr, F. et al. European emissions of mercury derived from long-term observations at Mace Head, on the western Irish coast"Atm.Env. 40, 6966-6974, 2006

Temme C. et al “Measurements of atmospheric mercury species at a coastal site in the antarctic and over the south atlantic ocean during polar summer” Env. Sci. Tech. 37, 22-31, 2003

Temme, C. et al “Trend, seasonal and multivariate analysis study of total gaseous mercury ata from the Canadian atmospheric mercury measurement network” Atm. Env. 41, 5423-5441, 2007.

LOTOS-EUROS

The LOTOS-EUROS model is a 3D chemistry transport model aimed to simulate air pollution in the lower troposphere. The model has been used for the assessment of particulate air pollution in a number of studies directed to total PM10 (Denby et al. 2008, Manders et al. 2009, van Zelm et al. 2008), secondary inorganic components (Barbu et al. 2008, Schaap et al. 2004b, Erisman et al., 2004), primary carbonaceous components (Schaap et al. 2004a, Schaap and van der Gon 2007) and trace metals (Denier van der Gon et al., 2008). The model has participated frequently in international model comparisons addressing ozone (Hass et al. 1997, van Loon et al. 2007) and particulate matter (Cuvelier et al. 2007, Hass et al. 2003, Stern et al. 2008, Schaap et al., 2009). For a detailed description of the model we refer to these studies as well as to the documentation of the model (Annex XVII, Schaap et al., 2005; 2009). Here, we describe briefly the model set-up used in MAPESI.

Model geometry

The domain of LOTOS-EUROS is bounded between 10°W to 40°E and 35°N to 70°N. The projection is normal longitude-latitude and the grid resolution is 0.5° longitude x 0.25° latitude, approximately 25 x 25 km. The model code is structured such that further zooming is possible. In the vertical there are currently three dynamic layers and a surface layer. The standard model version extends in vertical direction 3.5 km above sea level. The lowest dynamic layer is the mixing layer, followed by two reservoir layers. The height of the mixing layer is part of the diagnostic meteorological input data. The heights of the reservoir layers are determined by the difference between the mixing layer height and 3.5 km. Both reservoir layers are equally thick with a minimum of 50m. In some cases when the mixing layer extends near or above 3500 m the top of the model exceeds the 3500 m according to the above mentioned description. Simulations incorporate a surface layer of a fixed depth of 25 m. Hence, this layer is always part of the dynamic mixing layer. For output purposes the concentrations at measuring height (usually 3.6 m) are diagnosed by assuming that the flux is constant with height and equal to the deposition velocity times the concentration at height *z*.

Transport

The transport consists of advection in 3 dimensions, horizontal and vertical diffusion, and entrainment/detrainment. The advection is driven by meteorological fields (u,v) which are input every 3 hours. The vertical wind speed w is calculated by the model as a result of the divergence of the horizontal wind fields. The improved and highly-accurate, monotonic advection scheme developed by (Walcek, 2000) is used to solve the system. The number of steps within the advection scheme is chosen such that the courant restriction is fulfilled. Entrainment is caused by the growth of the mixing layer during the day. Each hour the vertical structure of the model is adjusted to the new mixing layer depth. After the new structure is set the pollutant concentrations are redistributed using linear interpolation. Vertical diffusion is described using the standard Kz theory. Vertical exchange is calculated employing the new integral scheme by (Yamartino et al., 2004).

Chemistry

In MAPESI, we use the TNO CBM-IV scheme which is a modified version of the original CBM-IV (Whitten et al., 1980). The scheme includes 28 species and 66 reactions, including 12 photolytic reactions. Compared to the original scheme steady state approximations were used to reduce the number of reactions. In addition, reaction rates have been updated regularly. The mechanism was tested against the results of an intercomparison presented by (Poppe et al., 1996) and found to be in good agreement with the results presented for the other mechanisms. We describe the N_2O_5 hydrolysis explicitly based on the available (wet) aerosol surface area (using $\gamma = 0.05$) (Schaap et al., 2004). Aqueous phase and heterogeneous formation of sulphate is described by a simple first oreder reaction constant (Schaap et al., 2004; Barbu et al., 2009). Aerosol chemistry is represented using ISORROPIA (Nenes et al., 1999).

Dry and wet deposition

The dry deposition in LOTOS-EUROS is parameterised following the well known resistance approach. The deposition speed is described as the reciprocal sum of three resistances: the aerodynamic resistance, the laminar layer resistance and the surface resistance. The aerodynamic resistance is dependent on atmospheric stability. The relevant stability parameters (u^*, L and Kz) are calculated using standard similarity theory profiles. The laminar layer resistance and the surface resistances for acidifying components and particles are described following the EDACS system (Erisman et al., 1994). Further down the dry deposition routine is described in more detail. Below cloud scavenging is described using simple scavenging coefficients for gases (Schaap et al., 2005) and following (Simpson et al., 2003) for particles. In-cloud scavenging is neglected due to the limited information on clouds. Neglecting in-cloud scavenging results in too low wet deposition fluxes (Annex IV, Comparison of the concentration and deposition data from LOTOS-EUROS and EMEP Unified Model) but has a very limited influence on ground level concentrations (see Schaap et al., 2004b).

Meteorological data

The LOTOS-EUROS system in its standard version is driven by 3-hourly meteorological data. These include 3D fields for wind direction, wind speed, temperature, humidity and density, substantiated by 2D gridded fields of mixing layer height, precipitation rates, cloud cover and several boundary layer and surface variables. LOTOS-EUROS can be run with different meteorological datasets. First is the meteorological data for Europe which is produced at the Freie Universität Berlin employing a diagnostic meteorological analysis system based on an optimum interpolation procedure on isentropic surfaces (TRAMPER). The TRAMPER-system utilizes all available synoptic surface and upper air data (Kerschbaumer and Reimer, 2003). Secondly, meteorological forecast data obtained from the European Centre for Medium-Range Weather Forecasts (ECMWF) can be used to force the model.

Within MAPESI we use ECMWF meteorology.

Emissions

The anthropogenic emissions used in this study are the PAREST emission data. These data are described in more detail in Denier van der Gon et al. (2010). The annual emission totals are broken down to hourly emission estimates using time factors for the emissions strength variation over the months, days of the week and the hours of the day. In LOTOS-EUROS biogenic isoprene emissions are calculated following the mathematical description of the temperature and light dependence of the isoprene emissions, proposed by (Guenther et al., 1993), using the actual meteorological data. In addition, sea salt emissions are parameterised following (Monahan et al.,1986) from the wind speed at ten meter height.

Land-use

The Corine/Smiatek data base has been enhanced using the tree species map for Europe made by (Koeble and Seufert, 2001), who also used Corine as a basis. This data base contains 115 tree species, on a grid of 1 x 1 km^2, with coverage per grid. In parts of the LOTOS-EUROS modeling domain, especially Russia, the Koeble tree map provides no information. We have coupled the Corine/Smiatek land use database to the database on tree species. In this procedure the land-use database was leading, meaning that tree species were only appointed to forest areas. In case no tree species information was available for a forest area, the three Corine forest categories are maintained. So, the full tree data base contains 115 + 3 categories. The combined database has a resolution of 0.0166° x 0.0166° which is aggregated to the required resolution during the start-up of a model simulation.

Dry deposition calculation

Several articles have reviewed the state of the science in evaluating dry deposition (Baldocchi, 1993; Erisman et al., 1994b; Erisman & Draaijers, 1995; Ruijgrok et al., 1995; Wesely & Hicks, 2000). Wesely and Hicks (2000) indicated that although models have been improving and can perform well at specific sites under certain conditions, there remain many problems and more research is needed. In spite of these problems, given the necessary meteorological and surface/vegetation data, there are a number of models for estimating deposition velocity (*Vd*) that have been shown to produce reasonable results using currently available information. Dry deposition processes for gaseous species are generally understood better than for

particles. Several dry deposition model formulations have been reported in the literature. These include big-leaf models (Hicks et al., 1987; Baldocchi et al., 1987), multi-layer models (Baldocchi, 1988; Meyers et al., 1998) and general dry deposition models (Erisman et al., 1996). Some of these models have been developed for estimating *Vd* at specific sites and are used within the framework of monitoring networks (Clarke et al., 1997; Meyers et al., 1991). Computation of the dry deposition rate of a chemical species requires that the concentraion *c* of the substance of interest is known through model computations or measurement. In most modelling schemes,the mass flux density *F* is found as

$$F = -V_d(z) \cdot c(z)$$

where *c(z)* is the concentration at height *z* and V_d is the dry deposition velocity. Estimates of deposition velocities V_d constitute the primary output of dry deposition models, both for large-scale models and site-specific methods of inferring dry deposition from local observations of concentrations, meteorological conditions, and surface conditions (Chang et al., 1987; Ganzeveld and Lelieveld, 1995). *z* is the reference height above the surface. If the surface is covered with vegetation, a zero-plane displacement is included: *z=z-d. d* is usually taken as 0.6-0.8 times the vegetation height .The absorbing surface is often assumed to have zero surface concentration and the flux is therefore viewed as being linearly dependent on atmospheric concentration. This holds only for depositing gases and not for gases that might be also emitted, such as NH_3 and NO. For these gases a nonzero surface concentration, a compensation point c_p, might exist, which can be higher than the ambient concentration, in which case the gas is emitted. For these gases the flux is estimated as

$$F = -V_d(z) \cdot [c(z) - c_p]$$

V_d provides a measure of conductivity of the atmosphere-surface combination for the gas and it is widely used to parameterise gas uptake at the ground surface (Wesely & Hicks, 2000). To describe the exchange of a range of gases and particles with very different chemical and physical properties, a common framework is provided, the resistance analogy (Wesely & Hicks, 2000). In this framework, V_d is calculated as the inverse of three resistances:

$$V_d(z) = \frac{1}{R_a(z-d) + R_b + R_c}$$

The three resistances represent bulk properties of the lower atmosphere or surface. R_a, R_b and R_c must be described by parameterisations. Although this approach is practical, it can lead to oversimplification of the physical, chemical, and biological properties of the atmosphere or surface that affect deposition.

The term R_a represents the aerodynamic resistance above the surface for the turbulent layer. R_a is governed by micrometeorological parameters and has the same value for all substances. R_a depends mainly on the local atmospheric turbulence intensities. Turbulence may be generated through mechanical forces of friction with the underlying surface (forced convection) or through surface heating (buoyancy or free convection). Unless wind speed is very low, free convection is small compared to mechanical turbulence.

The term R_b represents the quasi-laminar resistance to transport through the thin layer of air in contact with surface elements, and is governed by diffusivity of the gaseous species and air viscosity. For surfaces with bluff roughness elements, values of R_b are considerably larger than for relatively permeable, uniform vegetative cover, and the appropriate formulations should be used (Tuovinen et al., 1998).

Considerable variation from model to model is associated with the methods used to evaluate the surface or canopy resistance R_c for the receptor itself. R_c represents the capacity for a surface to act as a sink for a particular pollutant, and depends on the primary pathways for uptake such as diffusion through leaf stomata, uptake by the leaf cuticular membrane, and deposition to the soil surface. This makes R_c complicated, because it depends on the nature of the surface, the characteristics of the pollutant, and how the sink capacities for specific surfaces vary as a function of the local microclimate.

The resistance analogy is not used for particles. For sub-micron particles, the transport through the boundary layer is more or less the same as for gases. However, transport of particles through the quasi-laminar layer can differ. Whereas gases are transported primarily through molecular diffusion, particle

transport and deposition basically take place through sedimentation, interception, impaction and/or Brownian diffusion. Sedimentation under the influence of gravity is especially significant for receptor surfaces with horizontally oriented components. Interception occurs if particles moving in the mean air motion pass sufficiently close to an obstacle to collide with it. Like interception, impaction occurs when there are changes in the direction of airflow, but unlike interception a particle subject to impaction leaves the air streamline and crosses the quasi-laminar boundary layer with inertial energy imparted from the mean airflow. The driving force for Brownian diffusion transport is the random thermal energy of molecules.

Transport is a function of atmospheric conditions, characteristics of the depositing contaminant and the magnitude of the concentration gradient over the quasi-laminar layer (Davidson and Wu, 1990). Which type of transport process dominates is largely controlled by the size distribution of the particles (Slinn, 1982). For particles with a diameter <0.1μm, deposition is controlled by diffusion, whereas deposition of particles with a diameter >10μm is more controlled by sedimentation. Deposition of particles with a diameter between 0.1 and 1μm is determined by the rates of impaction and interception and depends heavily on the turbulence intensity. To describe particle dry deposition, the terms $(R_b+R_c)^{-1}$ on the right-hand side of Equation (2.3) must be replaced with a surface deposition velocity or conductance, and gravitational settings must be handled properly.

Dry deposition models or modules require several types of inputs from observations or from simulations of atmospheric chemistry, meteorology, and surface conditions. To compute fluxes, the concentrations of the substances must be known. Inputs required from meteorological models are values of friction velocity u^*, atmospheric stability via the Monin-Obukhov length scale L, aerodynamic surface roughness z_0, and aerodynamic displacement height d. Most dry deposition models also need solar radiation or, preferably, photosynthetically active radiation (PAR); ambient air temperature at a specified height; and measures of surface wetness caused by rain and dewfall. All models require a description of surface conditions, but the level of detail depends on the model chosen. Descriptions could include broad land use categories, plant species, leaf area index (LAI), greenness as indicated by the normalised difference vegetation index, various measures of plant structure, amount of bare soil exposed, and soil pH.

Land use dependent deposition; friction velocity and aerodynamic resistance

The atmospheric resistance to transport of gases across the constant flux layer is assumed to be similar to that of heat . R_a is approximated following the procedures used by Garland (1978):

$$R_{a,lu}(z_{ref} - d_{lu}) = \frac{1}{\kappa . u_{lu}^*} . \underbrace{\left[\ln\left(\frac{z_{ref} - d_{lu}}{z_{0,lu}}\right) + \Psi\left(\frac{z_{ref} - d_{lu}}{L}\right) + \Psi\left(\frac{z_{0,lu}}{L}\right) \right]}_{f(z_{ref} - d_{lu}, z_{o,lu}, L)} .$$

in which κ is the Von Karman constant (0.4), u^* is the friction velocity, which is calculated from the output of the meteorological model, L is the Monin-Obukhov length, d is the displacement height and z_0 is the roughness length, which is defined independently for each land use and season category. $\psi_h[(z-d)/L]$ is the integrated stability function for heat. These can be estimated using procedures described in Beljaars and Holtslag (1990). Under the same meteorological conditions, the aerodynamic resistance is the same for all gases and in fact also for aerosols. Only for aerosols with a radius > 5μm does the additional contribution of gravitational settling become significant. When the wind speed increases, the turbulence usually increases as well and consequently R_a becomes smaller.

To calculate the land use dependent aerodynamic resistance, it is needed to know the land-use specific u* and z0. The roughness length z0 is a given input parameter. Normally, the gridcell average, land use independent, u* is calculated from the wind speed at 10m (ECMWF input variable, 3 hourly) using stability formulations.

$$u_* = \frac{k u_{10\,m}}{\int_{z_{0,m}}^{z_{ref}} \phi_m \frac{dz}{z}}$$

To deduce a land use specific friction velocity, we need to rescale u*. To do this, we assume that at a height of 50m above the surface the wind speed is no longer land use dependent. On this assumption, we infer the wind speed at 50m height above the surface by using the calculated grid cell composite friction velocity and develop the stability formulation to a height of 50m above the surface. Afterwards, we again apply the same formulation, but now with a land use specific roughness length, and correcting for tree height where necessary, to infer the land use specific friction velocity.

Quasi laminar layer resistance

The second atmospheric resistance component R_b is associated with transfer through the quasi-laminar layer in contact with the surface. The transport through the quasi-laminar boundary layer takes place for gases by molecular diffusion and for particles by several processes: Brownian diffusion, interception, impaction and by transport under influence of gravitation. None of the processes for particles are as efficient as the molecular diffusion of gas molecules. This is because molecules are much smaller than aerosols and therefore have much higher velocities. For particles with radii <0.1μm Brownian diffusion is the most efficient process, whereas impaction and interception are relatively important for those with radii >1μm. For particles with radii between 0.1 and 1μm the transport through the quasi-laminar boundary layer is slowest (R_b is largest). The quasi-laminar boundary layer resistance is for most surface types more or less constant (forest, at sea for a wind speed < 3m/s) or decreases with wind speed (low vegetation).

R_b quantifies the way in which pollutant or heat transfer differs from momentum transfer in the immediate vicinity of the surface. The quasi-laminar layer resistance R_b can be approximated by the procedure presented by Hicks et al. (1987):

$$R_b = \frac{2}{\kappa \cdot u_*} \cdot \left(\frac{Sc}{\mathrm{Pr}} \right)^{2/3}$$

where *Sc* and *Pr* are the Schmidt and Prandtl number, respectively. *Pr* is 0.72 and *Sc* is defined as $Sc = \upsilon / D_i$, with υ being the kinematic viscosity of air (0.15 $cm^2\ s^{-1}$) and D_i the molecular diffusivity of pollutant *i* and thus component specific. The Schmidt and Prandtl number correction in the equation for R_b is listed in Table 2.1 for different gases. Molecular and Brownian diffusivities for a selected range of pollutants, and the deduced values of Schmidt number are listed in Table 2.1. Usually R_b values are smaller than R_a and R_c. Over very rough surfaces such as forest canopies, however, R_a may approach small values and the accuracy of the R_b estimate becomes important. This is especially the case for trace gases with a small or zero surface resistance.

Table 2.1: Schmidt and Prandtl number correction in equation for R_b (Hicks et al., 1987) for different gaseous species, and the diffusion coefficient ratio of water to the pollutant *i* (Perry, 1950).

Component	$D^*_{H_2O} / D_i$	**$(Sc/Pr)^{2/3}$**
SO_2	1.9	1.34
NO	1.5	1.14
NO_2	1.6	1.19
NH_3	1	0.87
HNO_2	1.7	1.24
HNO_3	1.9	1.34
HCl	1.5	1.14
PAN	2.8	1.73
H_2O	1	0.87
O_3	1.5	1.14

$$D_{H_2O} = 2.27 \cdot 10^{-5}\ m^2\ s^{-1}$$

Table 2.2 Molecular (for gases) and Brownian (for particles) diffusivities (D; $cm^2\ s^{-1}$) for a range of pollutants, and the deduced values of Schmidt number (Sc). The viscosity of air is taken to be 0.15 $cm^2\ s^{-1}$. From Hicks et al. (1987).

Component	***D***	***Sc***
Gaseous species		
H_2	0.67	0.22
H_2O	0.22	0.68
O_2	0.17	0.88
CO_2	0.14	1.07
NO_2	0.14	1.07
O_3	0.14	1.07
HNO_3	0.12	1.25
SO_2	0.12	1.25
Particles (unit density)		
0.001 μm radius	$1.28\ 10^{-2}$	$1.17\ 10^{1}$
0.01	$1.35\ 10^{-4}$	$1.11\ 10^{3}$
0.1	$2.21\ 10^{-6}$	$6.79\ 10^{4}$
1	$1.27\ 10^{-7}$	$1.18\ 10^{6}$
10	$1.38\ 10^{-8}$	10^{7}

Surface resistance

The surface or canopy resistance R_c is the most difficult of the three resistances to describe, and is often the controlling resistance of deposition flux. The analytical description of R_c has been difficult since it involves physical, chemical and biological interaction of the pollutant with the deposition surface. Over a given area of land, numerous plant, soil, water, and other material surfaces are present, each with a characteristic resistance to uptake of a given pollutant.

R_c values presented in the literature are primarily based on measurements of V_d and on chamber studies. By determining R_a and R_b from the meteorological measurements, R_c can be calculated as the residual resistance. Values of R_c can then be related to surface conditions, time of day, etc., yielding parameterisations. However, measurements using existing techniques are still neither accurate nor complete enough to obtain R_c values under most conditions. Furthermore, R_c is specific for a given combination of pollutants, type of vegetation and surface conditions, and measurements are available only for a limited number of combinations.

The surface resistance of gases consists of other resistances (Figure 2.1), either determined by the actual state of the receptor, or by a memory effect. R_c is a function of the canopy stomatal resistance R_{stom} and mesophyll resistance R_m; the canopy cuticle or external leaf resistance R_{ext}; the soil resistance R_{soil} and in-canopy resistance R_{inc}, and the resistance to surface waters or moorland pools R_{wat}. In turn, these resistances are affected by leaf area, stomatal physiology, soil and external leaf surface pH, and presence and chemistry of liquid drops and films. Based on values from the literature for the stomatal resistance (Wesely, 1989), and on estimated values for wet (due to rain and to an increase in relative humidity) and snow-covered surfaces, the parameterisation by Erisman et al (1994) (with the stomatal resistance, external leaf surface resistance and soil resistance acting in parallel) is used in LOTOS-EUROS. The parameterisation is given below and illustrated in Fig 2.2. For a description of the resistances that determines the Rc value we refer to Erisman et al. (1994).

vegetative surface:

$$R_c = \left[\frac{1}{R_{stom} + R_m} + \frac{1}{R_{inc} + R_{soil}} + \frac{1}{R_{ext}} \right]^{-1} \quad (2.1)$$

water surfaces:

$$R_c = R_{wat} \quad (2.2)$$

bare soil:

$$R_c = R_{soil} \quad (2.3)$$

snow cover:

$$R_c = R_{snow} \quad (2.4)$$

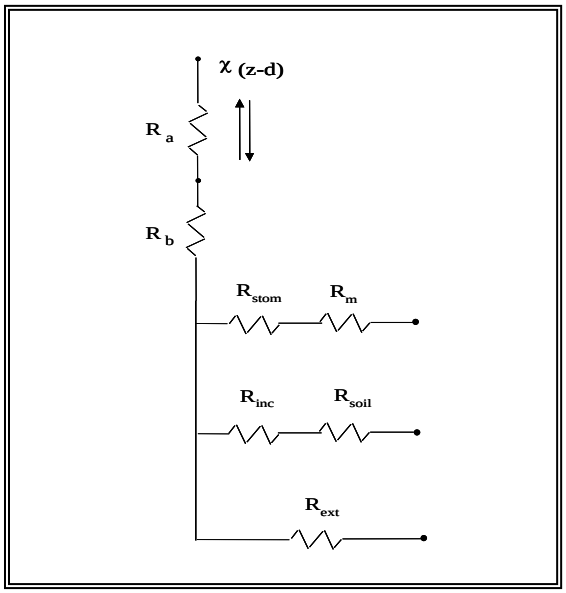

Figure 2.2 Resistance analogy approach in the dry deposition module

Simulation set-up

For MAPESI we have performed a two-step approach to calculate the dry deposition fluxes over Germany for 2004-2007. First, we have performed simulations on a European domain bound at 35° and 70° North and 10° West and 40° East. The grid resolution in this domain is 0.50° longitude x 0.25° latitude, which is approximately 25 x 25 km² over Germany. Second, we used the one-way zoom option for a high resolution simulation over Germany and its direct surroundings with an increase in resolution of a factor 4. In this way we obtain a high resolution simulation over Germany with consistent boundary conditions from the European domain to take the long range transport of pollutants into account. The meteorological driver used in MAPESI is obtained from ECMWF. Anthropogenic emissions are obtained from the PAREST project (Jörß et al., 2010).

References

Baldocchi, D.D., Hicks, B.B. and Camara, P. (1987). A canopy stomatal resistance model for gaseous deposition to vegetated surfaces. Atmospheric Environment 21, 91-101.

Baldocchi, D.D., Hicks, B.B., Meyers, T.P. (1988). Measuring biosphere-atmosphere exchanges of biologically related gases with micrometeorological methods. Ecology 69, 1331-1340.

Baldocchi, D.D. (1993). Deposition of gaseous sulfur compounds to vegetation. In Sulfur Nutrition and Assimilation and Higher Plants (eds. Kok, L.J. et al.), pp. 271-293, SGP Academic, The Hauge, Netherlands.

Beljaars, A.C.M. and Holtslag, A.A.M. (1990). Description of a software library for the calculation of surface fluxes. Environ. Software 5, 60-68.

Chang, J.C., Brost, R.A., Isaksen, I.S.A., Madronich, P., Middleton, P., Stockwell, W.R. and Walcek, C.J. (1987). A three-dimensional Eulerian acid deposition model: physical concepts and formulation. Journal of Geophysical Research 92, 14681-14700.

Davidson, C.I. and Wu, Y.L. (1990). Dry deposition of particles and vapors. In Acidic Precipitation (eds. S.E. Lindberg, A.L. Page and S.A. Norton), vol. 3. Springer-Verlag, New York.

Erisman, J.W., Pul, A. van and Wyers, P. (1994b). Parameterization of surface resistance for the quantification of atmospheric deposition of acidifying pollutants and ozone. Atmospheric Environment 28(16), 2595-2607.

Erisman, J.W. and Draaijers, G.P.J. (1995). Atmospheric deposition in relation to acidification and eutrophication. Elsevier, New York.

Erisman, J.W., Mennen, M.G., Fowler, D., Flechard, C.R., Spindler, G., Grüner, Duyzer, J.H., Ruigrok, W. and Wyers, G.P. (1996). Towards development of a deposition monitoring network for air pollution of Europe. RIVM Report no. 722108015, National Institute of Public Health and the Environment, Bilthoven, The Netherlands, April 1996.

Ganzeveld, L. and Lelieveld, J. (1995). Dry deposition parameterization in a chemistry general circulation model and its influence on the distribution of reactive trace gases. Journal of Geophysical Research 100, 20999-21012.

Hass, H., van Loon, M., Kessler, C., Stern, R., Matthijsen, J., Sauter, F., Zlatev, Z., Langner, J., Foltescu, V. and Schaap, M. (2003) 'Aerosol modelling: Results and Intercomparison from European Regional – scale modelling systems', *Special Rep. EUROTRAC-2 ISS*, Munchen.

Hicks, B.B., Baldocchi, D.D., Meyers, T.P., Hosker Jr, R.P. and Matt, D.R. (1987). A preliminary multiple resistance routine for deriving dry deposition velocities from measured quantities. Water Air Soil Pollut. 36, 311-330.

Kerschbaumer, A. and Reimer, E. (2003) 'Preparation of Meteorological input data for the RCG-model', *UBA-Rep. 299 43246,* Free Univ. Berlin Inst for Meteorology (in German).

Meyers, T.P., Finklestein, P., Clarke, J., Ellestad, T. and Sims, P.F. (1998). A multi-layer model for inferring dry deposition using standard meteorological measurements. Journal of Geophysical Research 103, 22645-22661.

Monahan, E.C., Spiel, D.E., Davidson, K.L. (1986) 'A model of marine aerosol generation via whitecaps and wave disruption', In *Oceanic Whitecaps and their role in air/sea exchange*, edited by Monahan, E.C, and Mac Niocaill, G., pp. 167-174, D. Reidel, Norwell, Mass., USA

Nenes, A., Pilinis, C., and Pandis, S. N. (1999) 'Continued Development and Testing of a New Thermodynamic Aerosol Module for Urban and Regional Air Quality Models', Atmos. *Env.*, Vol. 33 , pp.1553-1560.

Poppe, D., Andersson-Sköld, Y., Baart, A., Builtjes, P.J.H., Das, M., Fiedler, F., Hov, O., Kirchner, F., Kuhn, M., Makar, P.A., Milford, J.B., Roemer, M.G.M., Ruhnke, R., Simpson, D., Stockwell, W.R., Strand, A., Vogel, B., Vogel, H. (1996) 'Gas-phase reactions in atmospheric chemistry and transport models: a model intercomparison*', Eurotrac report. ISS*, Garmisch-Partenkirchen.Nenes A., Pilinis, C.,

Pandis, S.N. (1998), Isorropia: A new thermodynamic model for multiphase multicomponent inorganic aerosols, Aquatic Geochemistry, 4, 123-152

Ruijgrok, W., Davidson, C.I. and Nicholson, K.W. (1995). Dry deposition of particles. Implications and recommendations for mapping of deposition over Europe. Tellus 47B, 587-601.

Schaap, M., van Loon, M., ten Brink, H.M., Dentener, F.D., Builtjes, P.J.H. (2004a) 'Secondary inorganic aerosol simulations for Europe with special attention to nitrate', *Atmos. Phys. Chem*., Vol. 4, pp.857-874

Schaap, M., Denier Van Der Gon, H.A.C., Dentener, F.J., Visschedijk, A.J.H., van Loon, M., Ten Brink, H.M., Putaud, J-P., Guillaume, B., Liousse, C. and Builtjes, P.J.H. (2004c) 'Anthropogenic Black Carbon and Fine Aerosol Distribution over Europe', *J. Geophys. Res.*, Vol. 109, D18201, doi: 10.1029/2003JD004330.

Schaap, M., M. Roemer, F. Sauter, G. Boersen, R. Timmermans, P.J.H. Builtjes (2005), LOTOS-EUROS Documentation, TNO report B&O 2005/297, TNO, Apeldoorn, the Netherlands.

Simpson, D., Fagerli, H., Jonson, J.E., Tsyro, S., Wind, P., and Tuovinen, J-P (2003) 'Transboundary Acidification, Eutrophication and Ground Level Ozone in Europe, Part 1: Unified EMEP Model Description', *EMEP Report 1/2003*, Norwegian Meteorological Institute, Oslo, Norway.

Slinn, W.G.N. (1982). Predictions for particle deposition to vegetative surfaces. Atmospheric Environment 16, 1785-1794

Tuovinen, J.P., Aurela, M. and Laurila, T. (1998). Resistances to ozone deposition to flark fen in the northern aapa mire zone. Journal of Geophysical Research 103, 16953-16966.

Wesely, M.L. (1989). Parameterization of surface resistances to gaseous dry deposition in regional-scale numerical models. Atmospheric Environment 23, 1293-1304

Wesely, M.L. and Hicks, B.B. (2000). A review of the current status of knowledge on dry deposition. Atmospheric Environment 34, 2261-2282.

Whitten, G., Hogo, H., Killus, J. (1980) 'The Carbon Bond Mechanism for photochemical smog', *Env. Sci. Techn*., Vol. 14, pp.14690-14700.

Yamartino, R. J., Flemming, J. and Stern, R.M. (2004) 'Adaption of analytic diffusivity formulations to eulerian grid model layers finite thickness', *27th ITM on Air Pollution Modelling and its Application.* Banff, Canada, October 24-29, 2004.

Evaluation of the calculated concentrations by LOTOS-EUROS and the calculation of the dry deposition of N- and S-species

In Figure 3.1 and 3.2 we show the modelled annual average distributions of acidifying components over Germany for 2005. First we shortly discuss the distribution of the primary components. Ammonia emissions and concentrations are highest in the north western part of the country, including Nieder-Sachsen, Nord-Rhein-Westfalen. Secondary maxima are found over the southern part of the country in Bayern and Baden-Wurttemberg. Low concentrations are modelled in a region over central Germany including Rheinland, Hessen and eastern Germany. Sulphur dioxide originates mainly from combustion of sulphur containing fuels in power plants. The concentrations are highest (> 8 $\mu g/m^3$) around the Ruhr area as well as major industrial and harbour cities. Over most of the country concentrations between 2 and 4 $\mu g/m^3$ are modelled. Note the impact of international shipping at the North Sea and the Nord-Ostsee-Kanal. The annual average concentrations of NO and NO2 maximise over densely populated areas. The Ruhr-area and large cities such as Berlin, Munich and Stuttgart are recognised in the distributions. In those areas NO2 concentrations exceed 15 $\mu g/m^3$. NO concentrations are generally lower than NO2 and are highest during night time.
The concentration distributions for the secondary components are much more even. This is especially the case for sulphate. Over Europe sulphate concentrations show a large scale pattern with highest concentrations over south-eastern Europe. Not surprisingly, modelled concentrations are highest outside Germany in Poland and Czech Republic. Within Germany concentration of about 2 $\mu g/m^3$ are modelled close to the border with the indicated countries as well as over the Ruhr area, the major source area for sulphur dioxide in the country. Over the remainder of the country the annual average concentrations are very similar with a variability of less than 0.3 $\mu g/m^3$. The mass concentrations of the particulate components are dominated by nitrate. Nitrate concentrations show a similar distribution over Germany as ammonia, although the gradients are less than for ammonia. The similarity in the distributions can be explained by the semi-volatile character of ammonium nitrate. In summer high ammonia levels are needed to maintain the equilibrium between the gas and aerosol phase and hence nitrate is only stable in areas with high ammonia concentrations. In winter ammonium nitrate is stable and is more evenly distributed over the country. Nitric acid concentrations show a field which is anti-correlated to that of ammonia. The reason is that the nitric acid in the high ammonia regions is in the form of particulate nitrate whereas it is in the gas phase in low ammonia areas. Ammonium is present as ammonium sulphate and ammonium nitrate. Hence, the distribution resembles that of the combined sulphate and nitrate.

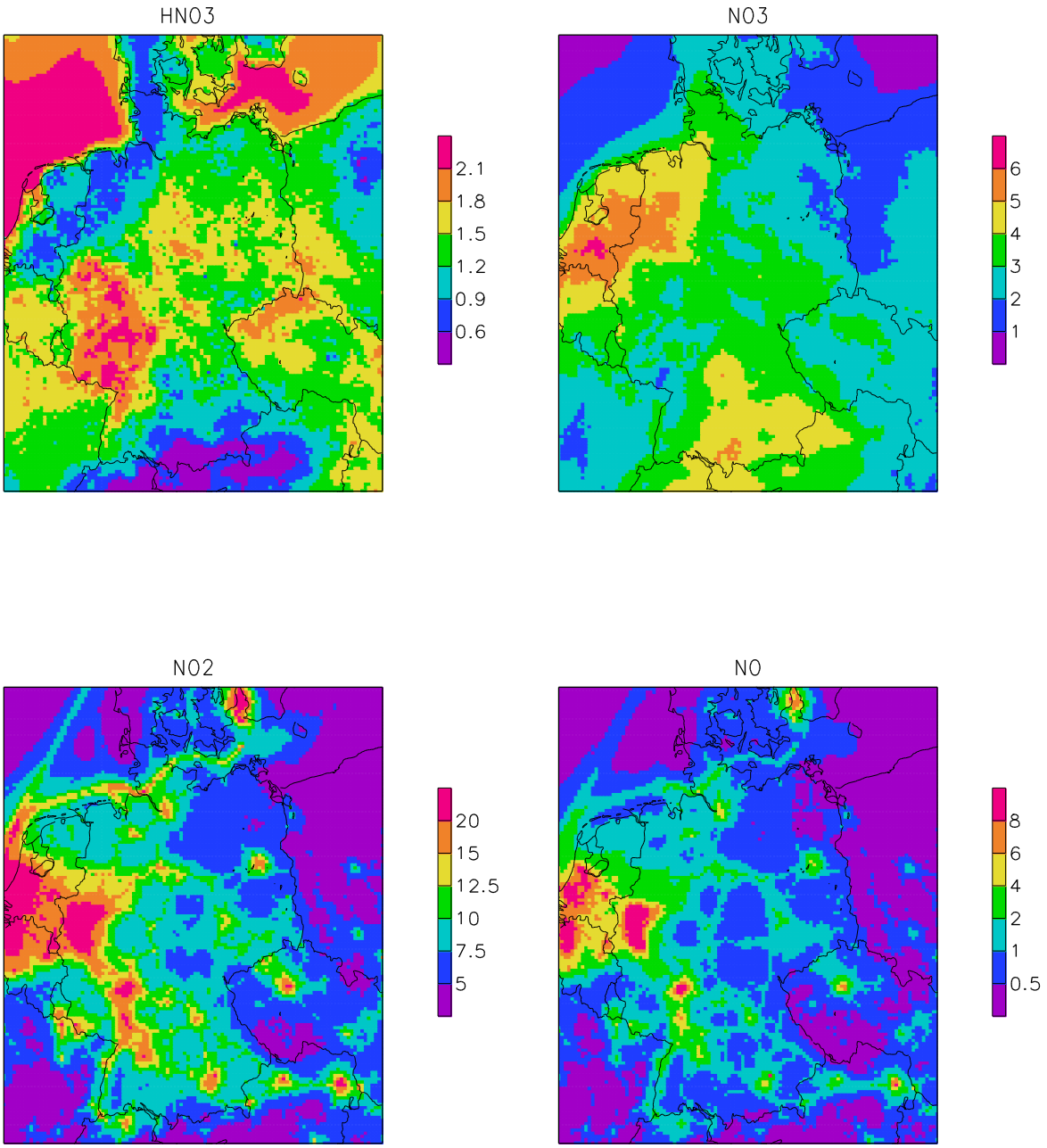

Figure 3.1. Annual average concentration fields (μg/m^3) for the oxidized nitrogen components nitric acid (HNO3), aerosol nitrate (NO3), nitrogen dioxide (NO2) and nitrogen oxide (NO).

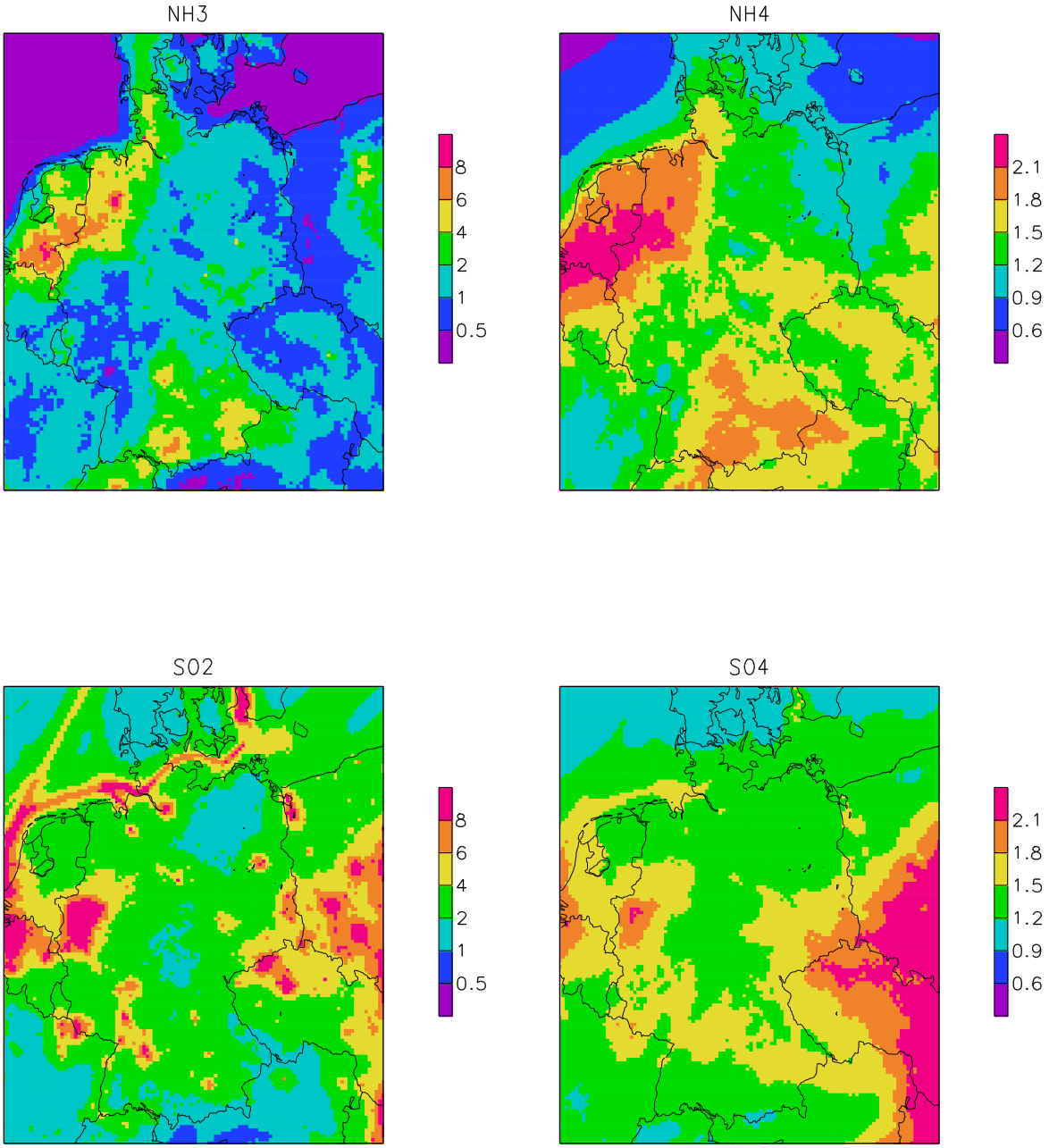

Figure 3.2. Annual average concentration fields (μg/m^3) for the reduced nitrogen and sulphur components ammonia (NH3), aerosol ammonium (NH4), sulphur dioxide (SO2) and aerosol sulphate (SO4).

Within the MAPESI project the deposition fluxes are calculated at an hour by hour basis. To evaluate the temporal behavior of the model we have compared the modeled daily mean concentrations against those measured at the German UBA stations. The comparison is summarized in the form of scatter plots. In these plots all data points are compared for all stations for 2005. The stations used are:

Station_ID	Lat	Lon	Height	Station_Name
DEUB033	51.52	12.9	86	Melpitz
DEUB030	53.15	13.03	65	Neuglobsow
DEUB028	54.43	12.73	1	Zingst
DEUB001	54.93	8.32	12	Westerland
DEUB002	49.76	7.06	480	Deuselbach
DEUB005	52.80	10.60	74	Waldhof
DENW102	51.48	6.73	28	Duisburg-Bruckhausen
DENW021	51.52	6.97	40	Bottrop-Wellheim
DE0002R	52.80	10.76	74	Langenbrügge
DE0003R	47.91	7.91	1205	Schauinsland
DE0005R	48.82	13.22	1016	Brotjacklriegel
DE0008R	50.65	10.77	937	Schmücke

In addition to the scatter plots we provide the time series for each component for the second half of the year 2005 at Neuglobsow.
Aerosol nitrate is difficult to measure due to the volatile character of ammonium nitrate and the reactivity of nitric acid. For monitoring purposes simple techniques are employed to measure the sum of particulate nitrate and nitric acid in a filter pack. Some problems arise in the determination of the partitioning of the nitrate over the gas and aerosol phase. Nitrate may evaporate from the first aerosol filter and adsorbed to the impregnated filter at temperature above 20 degrees Celcius. Hence, in summer aerosol nitrate may be underestimated and nitric acid overestimated. Despite these potential artefacts we provide a comparison for both aerosol nitrate and nitric acid.

LOTOS-EUROS is able to capture the variability in sulfur dioxide quite well. The temporal behavior corresponds well with the observed concentrations; many peaks are captured by the model. The modeled sulfate concentrations are systematically underestimated by about 50%. The temporal behavior is slightly less than that for sulfur dioxide. The underestimation of sulfate may imply that the formation efficiency is not high enough in the model. As the formation of sulfate in cloud water is difficult to parameterize and strongly dependent on cloud water pH an improvement of the description is under investigation.

Nitrate concentrations are slightly underestimated in the model. On the other hand, the nitric acid concentrations are slightly overestimated. The model captures the seasonal variation with lower nitrate concentrations in summer and higher concentrations in winter/spring quite well. The seasonal variation in nitric acid and nitrate can be explained by an effective transfer to the aerosol phase in winter due to the stability of ammonium nitrate in combination with a higher total availability of ammonia compared to nitrate (nitrate limiting ammonium nitrate formation) and more efficient photo-chemistry in combination with an unstable ammonium nitrate (higher partial pressure of ammonia) in summer.

At the rural background EMEP sites in Germany the modelled ammonium concentrations are in agreement with the observations. The spread in the scatter plot for ammonium and nitrate is larger than for sulfate. This may be explained by the dominant contribution of ammonium nitrate to ammonium and the more complex formation route of ammonium nitrate, yielding a larger variability around the mean.

In source areas the ammonia concentrations are underestimated significantly by the model. For example, at Zingst we underestimate by a factor 3. Also, the temporal correlation is low, especially in spring when the timing of the emissions is very difficult. In the model monthly mean (hourly) emission patters are assumed, whereas in reality the emissions occur in periods with intense agricultural activities (manure spreading). This is not a surprise given the resolution of the model and the siting of the stations. The

stations are located in agricultural areas with large ammonia emissions. Simulations on a higher resolution are needed. Now, comparing regional model results for sites located in agricultural areas is as if one compares a model result of NOx to a measurement in the centre of a large city.

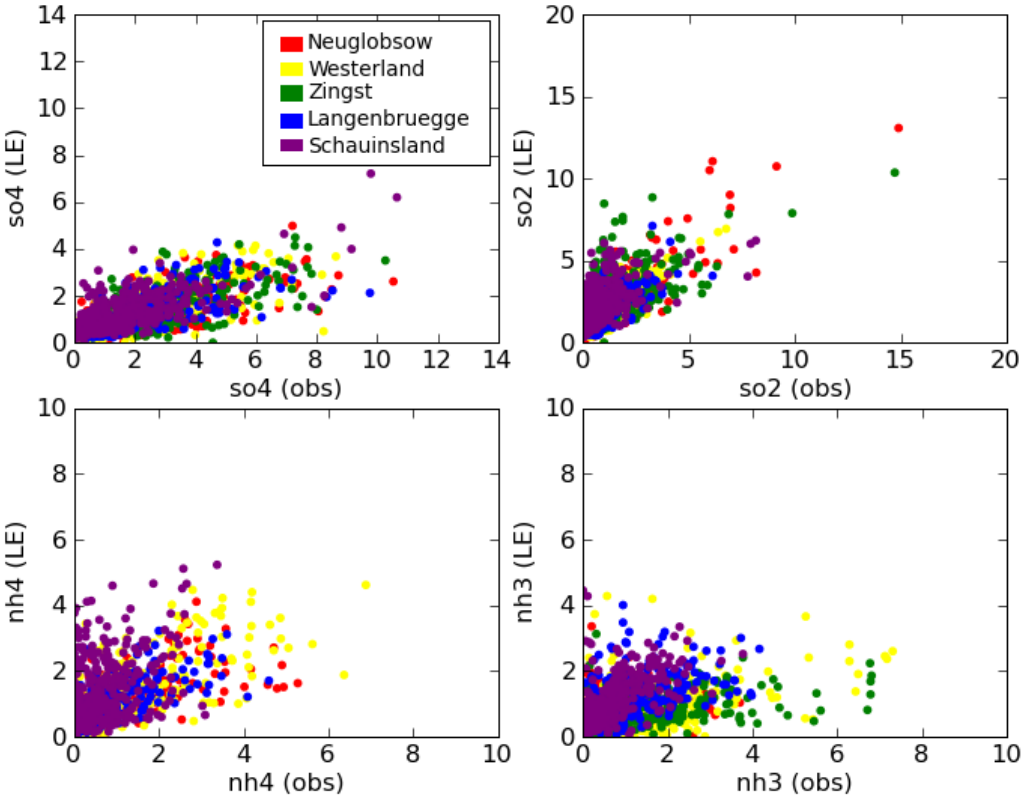

Figure 3.3 Comparison of observed and modeled (LE) daily average concentrations of Sulfur and reduced nitrogen components for 5 stations in 2005

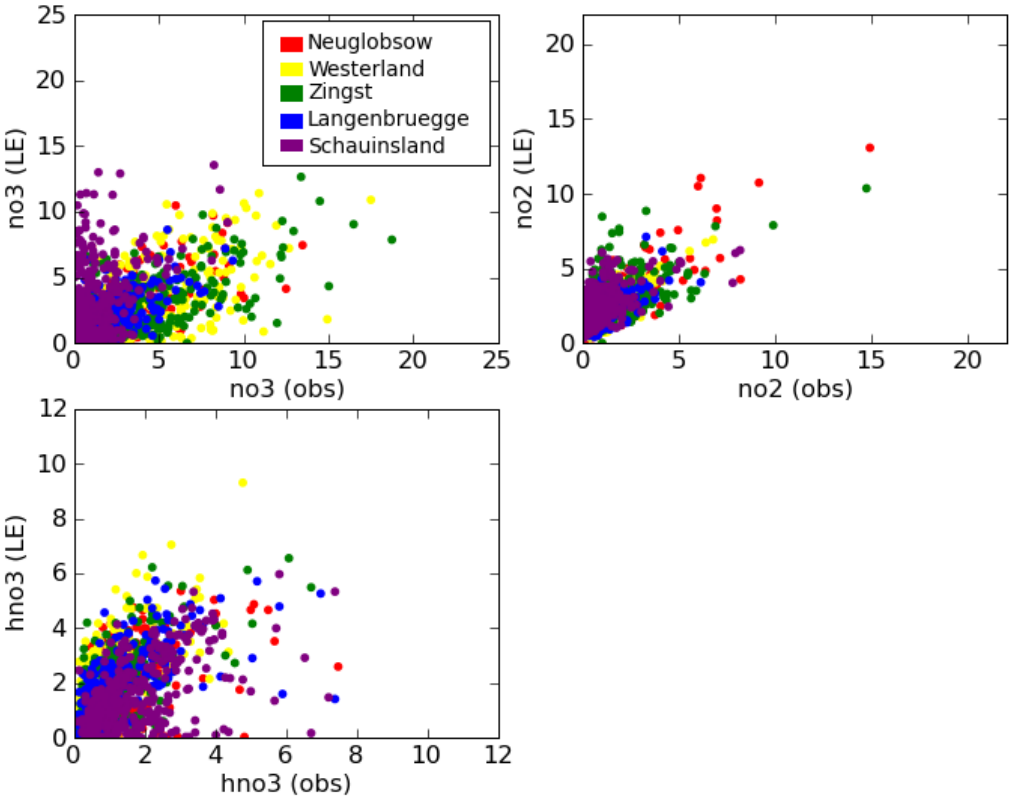

Figure 3.4 Comparison of observed and modeled (LE) daily average concentrations of oxidised nitrogen components for 5 stations in 2005

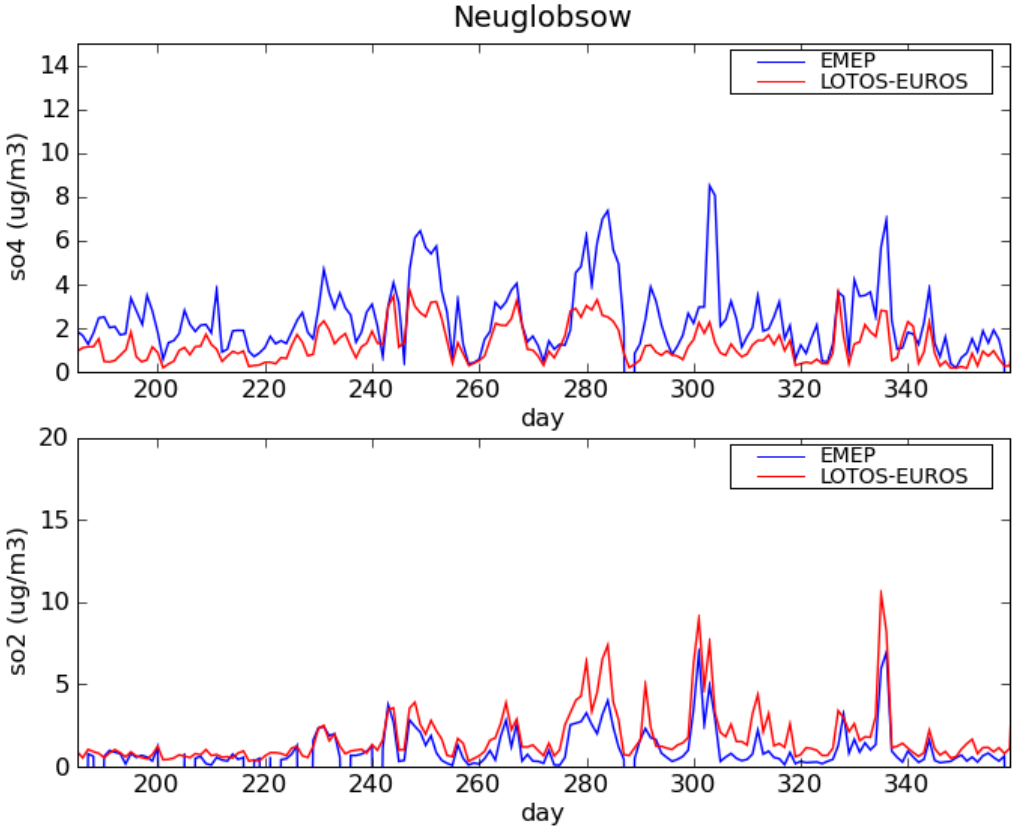

Figure 3.4 Comparison of observed and modeled (LE) daily average concentrations of sulfur components for Neuglobsow in the second half of 2005

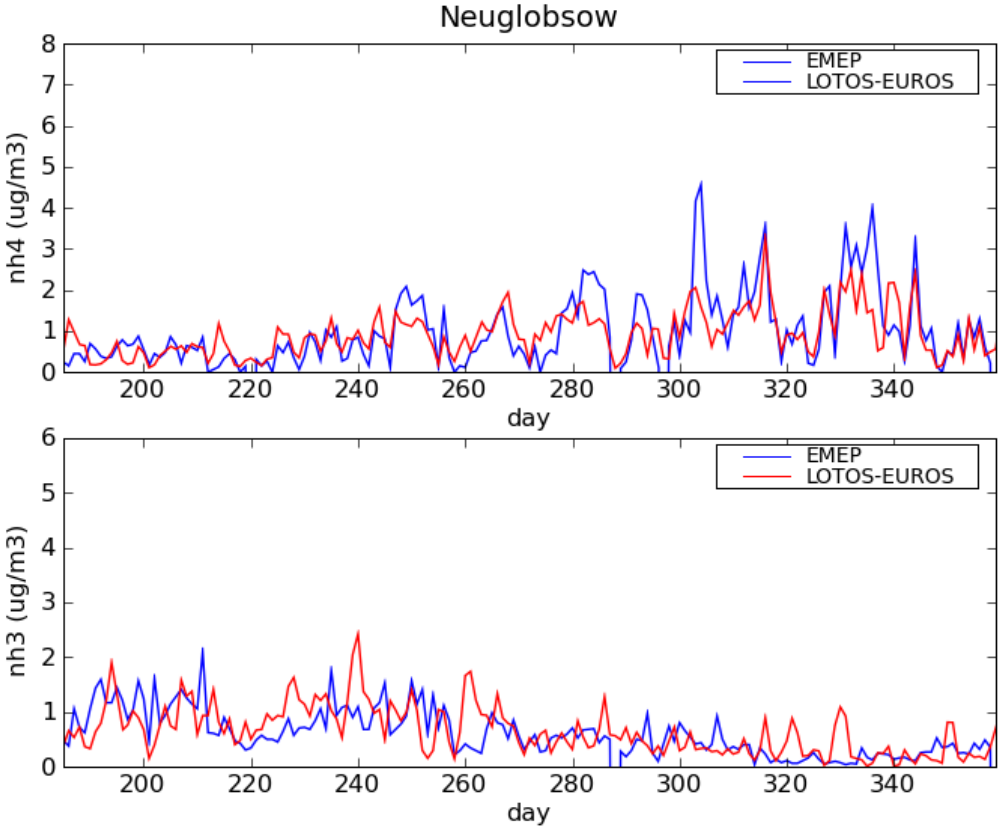

Figure 3.5 Comparison of observed and modeled (LE) daily average concentrations of reduced nitrogen components for Neuglobsow in the second half of 2005

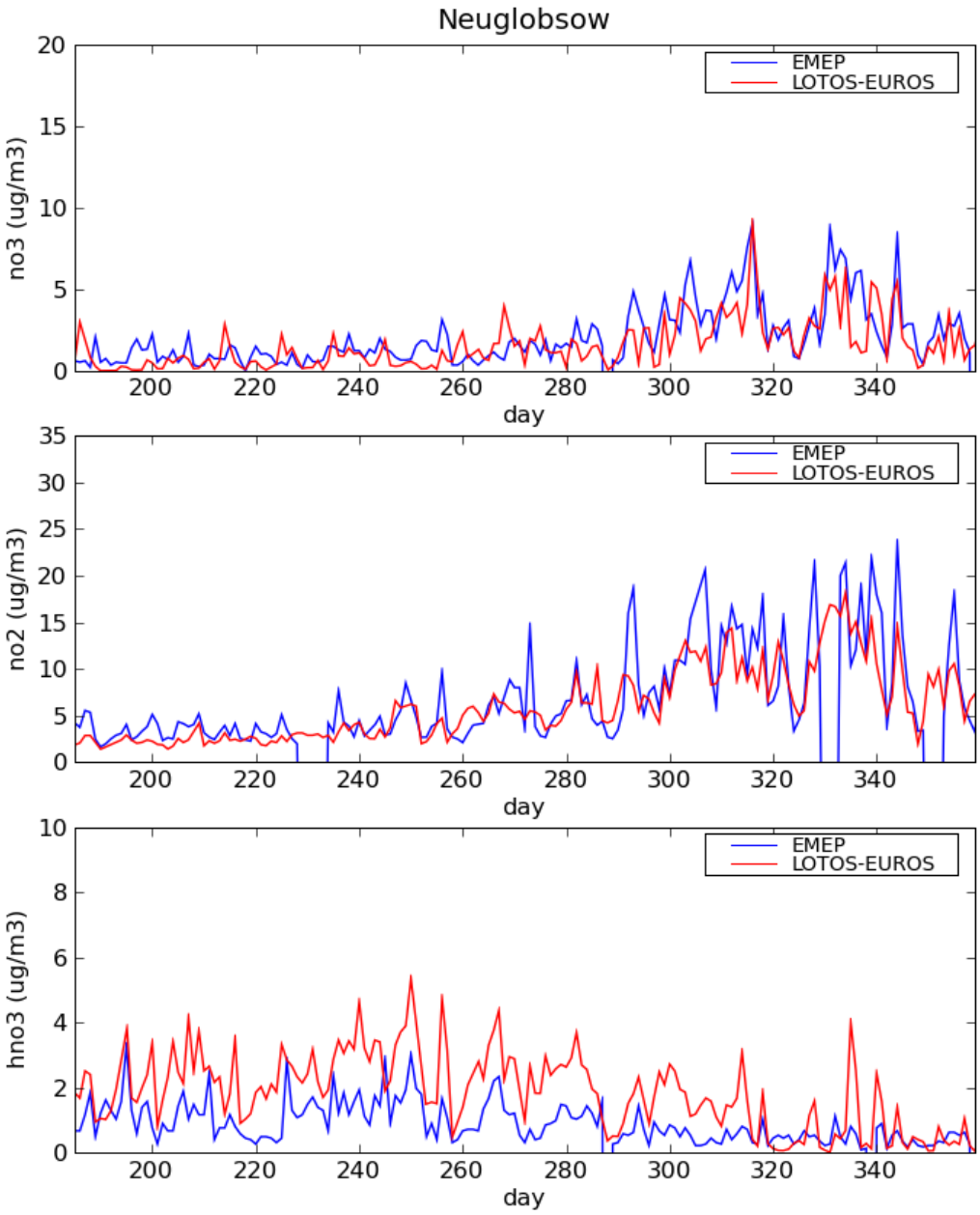

Figure 3.6 Comparison of observed and modeled (LE) daily average concentrations of oxidised nitrogen components for Neuglobsow in the second half of 2005

Modelled dry deposition fluxes

In this section we provide an overview of the modeled dry deposition fluxes for the years 2005-2007. As for the concentrations we will provide the distributions for 2005. The data for the other years are tabulated and presented in more detail in Paragraph 3.4 at a 1x1 Km^2 resolution.
In Figure 3.7 we present the annual total dry deposition distribution for sulphur and oxidized and reduced nitrogen. The distributions show the composite values, meaning that an hectare has the average land use distribution of that grid cell. The deposition flux for oxidized sulfur shows maxima in the Ruhr area, along the Nord-Ost-see canal, and some locations near large power plants or industrial complexes. Only in the Ruhr area the deposition flux exceeds 600 Eq ha^{-1} a^{-1}. On average the deposition flux is 214 Eq ha^{-1} a^{-1} over Germany. The dry deposition distribution of oxidized nitrogen resembles the distribution of nitric acid concentrations and no2 concentrations. Over central Germany a large scale background of about 200-300 Eq ha^{-1} a^{-1} is present. Maxima reach to values above 600 Eq ha^{-1} a^{-1}. On average over Germany the flux is 260 Eq ha^{-1} a^{-1}in the year 2005. The nitrogen input due to dry deposition is dominated by reduced nitrogen. On average the dry deposition flux for Germany is 511 Eq ha^{-1} a^{-1}, roughly two times the amount of oxidized nitrogen. Not surprisingly, the maxima are found in the areas with intensive agricultural activities, where ammonia emissions peak. In the southwest of Niedersachsen and the north of nordrhein-westfalen dry deposition fluxes exceed 1500 Eq ha^{-1} a^{-1}.
Comparison between the results for the three years learns that the variability between the years is rather small on average. The variability is highest for reduced nitrogen, a modest 10%, which may originate from differences in cross-border transport between Germany and the Netherlands. Note that the emissions for the years 2006 and 2007 have been interpolated between the PAREST- Base year Emissions of 2005 and das Referenz –Szenario 2010.

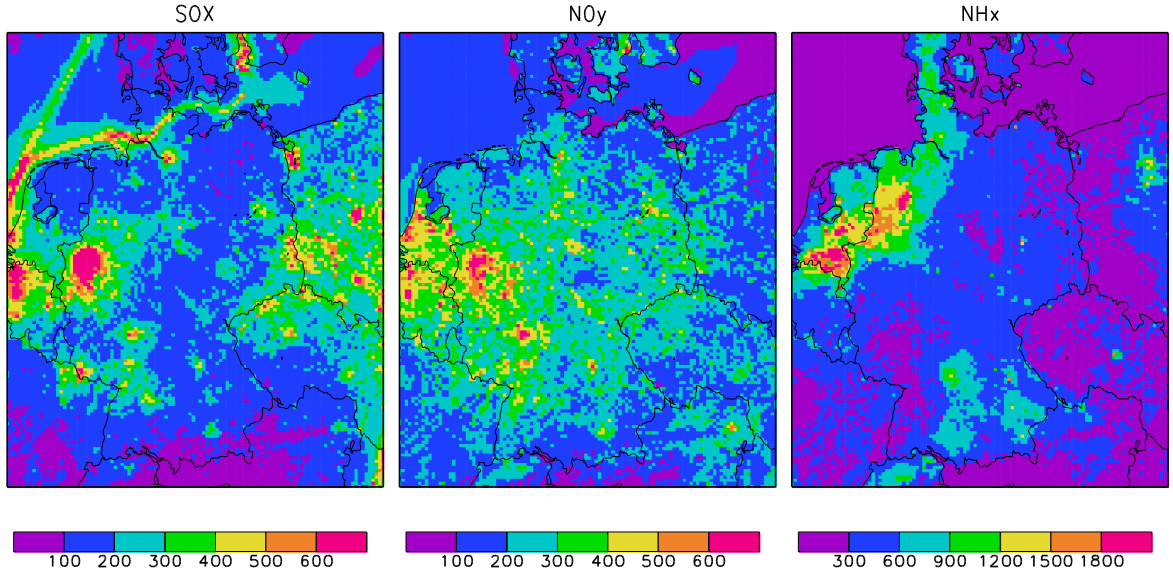

Figure 3.7 Annual dry deposition distributions for 2005 (Eq ha^{-1} a^{-1})

Table 3.5 . The average dry deposition flux (Eq ha^{-1} a^{-1}) for oxidized sulphur, oxidized nitrogen and reduced nitrogen.

Species	2005	2006	2007
SO_x	214	209	211
NO_y	260	259	250
NH_x	511	527	554
N-Gesamt	771	786	804

Dry deposition fluxes per land use category

To estimate the dry deposition fluxes at a 1 x 1 km^2 resolution the dry deposition fluxes per unit area to all land use categories should be known. These maps have been calculated for the whole of Germany. In Figure 3.8 and 3.9 we compare these distributions for grass land and deciduous forest for the components nitric acid and ammonia. See also the statistical description of modeling results of the different components and land use classes as presented in Annex XI

Nitric acid was selected as an example as the dry deposition velocity is basically determined by the variability in the aerodynamic resistance. As such the differences between the different land use classes can be interpreted as the consequence of the stability calculation per land use category. The ratio between the fluxes in a single cell (where concentrations are the same) is the ratio between the effective dry deposition velocities and for nitric acid by approximation the inverse ratio of the effective aerodynamic resistance.

Over Germany the distribution of the dry deposition fluxes are very similar for the different land use categories. This is driven by the concentration distributions that are a common driving force. For nitric acid the dry deposition fluxes are highest in the areas where nitric acid concentrations are high, which is the central part of the country where ammonia concentrations are quite low and nitrogen dioxide concentrations maximize. Comparing the fluxes to grass land and deciduous forest shows that the fluxes are significantly higher to forest than grassland. To forest the fluxes may be as high as 6 kg/ha/yr. In a relative sense the fluxes to forest are up to ninety percent higher than to grass in the southwest of the country. Minimum values of about 60% are found over the northwestern part of the country and the Netherlands. Over the remainder of Germany the central values appears to be 65 %.

For ammonia the deposition fluxes are larger than for nitric acid. Over rather large areas fluxes to forest are above 50 kg N per hectare per year. Even for grass land the maximum is about 50 kg N in the southwest of Niedersachsen. Over Germany the deciduous forest areas receive between 25 and 75% more NH_3-N than the grass land in the same cell. Highest ratios are found in the areas with relatively low ammonia levels and particularly in the regions with the highest SO_2 to NH_3 ratios. As a central value about 45% can be assumed.

The distribution of the ratio between forest and grass differs substantially from that of nitric acid. This means that these fields are difficult to compare. Different components have different seasonal variations and dependency on meteorology and area of origin. Concentrations and dry deposition velocities at a location are both dependent on meteorological conditions. Also, it means that when assessing the dry deposition flux for grass and forest in an experimental sense it is advisable to perform the experiments at a not too far distance from each other.

Note that we might very well underestimate the ratio of ammonia deposition between forest and grass land. The reason is that in reality the deposition flux is dependent on a compensation point. In the current model version however this compensation point is not taken into account explicitly yet and deposition and emission occur all the time simultaneously. Several studies show that the compensation point, which is more relevant over grass then over forest, might have an influence. However, the incorporation into the CTM's is still under discussion and subject to further investigations

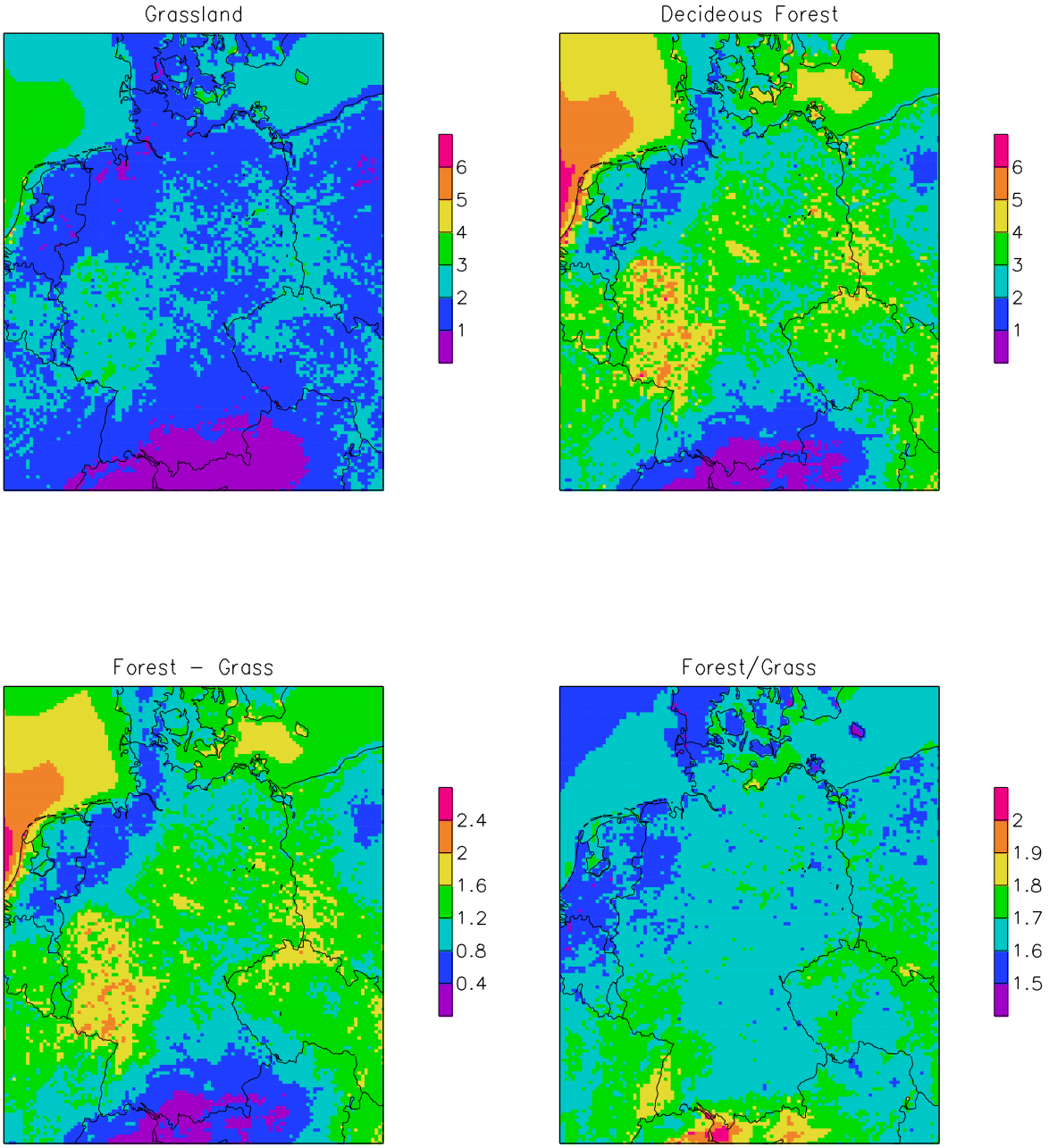

Figure 3.8. Comparison of the nitric acid dry deposition distribution for Grass land and Deciduous Forest. The panels show the annual total dry deposition for 2005 for grass land (upper left), the same for deciduous forest (upper right), the absolute difference between the two (lower left) and the relative Difference (lower right)

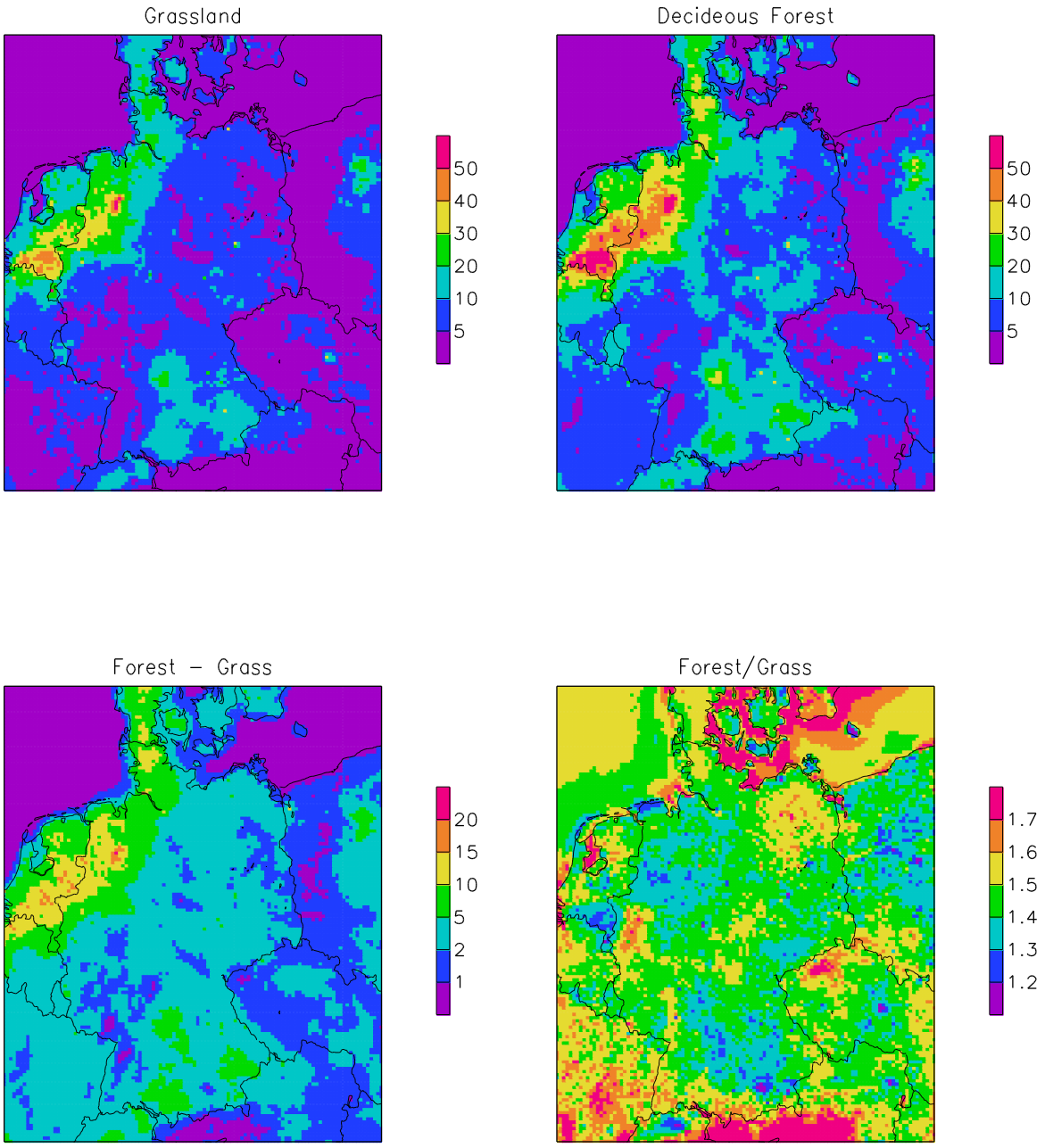

Figure 3.8. Comparison of the ammonia dry deposition distribution for Grass land and Deciduous Forest. The panels show the annual total dry deposition, for 2005, for grass land (upper left), the same for deciduous forest (upper right), the absolute difference between the two (lower left) and the relative Difference (lower right)

Sensitivity analysis

To investigate the overall uncertainty of the model results, three sensitivity analyses were performed to assess the sensitivities of the system. Results of these sensitivity runs were compared to the 2005 deposition results (Table 3.6 – Basis)

1.Sensitivity of dry deposition to the applied emission database;
Present calculated deposition ran with emission database PAREST2005 is compared with same model version ran with emission database used in previous project (TNO2004 Emissions). The differences seen for deposition fluxes are in line with the differences in the emission database, up to -15% ± 10% for SO_x,

-10% ± 10% for NO_y, and -5% ± 15% for NH_x over Germany (Table 3.6 – Emissions_2004). In the comparison between model runs for the year 2004 and 2005, the differences resulting from a different meteorology are smaller than those resulting from the differences in the applied emissions. It should be noted that this holds for the comparison between 2004 and 2005. When comparing with other years, like the year 2003, the results might well be different.

2.Sensitivity to roughness length

The land use specific roughness lengths as applied in the present calculations with LOTOS-EUROS differ from the roughness lengths as applied in the previous project, defined in IDEM. Overall, the roughness lengths as defined in IDEM are larger than the LOTOS-EUROS definitions, with main differences for land use classes arable land/permanent crops (0.25m vs. 0.075), semi-natural vegetation (0.25m vs. 0.1) and urban area (3.0m vs. 1.0), see also the description in paragraph 3.1. To get a feeling for the influence of the roughness length, calculations with LOTOS-EUROS have been performed by multiplying the LOTOS-EUROS roughness length by a factor 2.

This difference in roughness length will not directly be comparable to the difference between the dry deposition fluxes as calculated presently with LOTOS-EUROS and the results obtained in the previous project. A larger roughness length in LE will result in a larger deposition velocity so also in a lower concentration, which partly compensates the larger deposition flux .

So the differences found in this sensitivity run will be smaller than the differences between this project and the previous project

To estimate the sensitivity of the dry deposition to roughness length, the deposition flux calculations with the LOTOS-EUROS model in the present setup, but with the roughness length multiplied by a factor 2 were compared against the dry deposition fluxes as calculated in the standard model setup. Overall, and as expected, the calculation with the larger roughness lengths resulted in a higher deposition, i.e. 5-10% for all species on basis of annual total deposition, with evenly distributed variation throughout Germany (Table 3.6 – z_0).

3.Sensitivity to tree height

In the standard model setup, the effect of displacement height is only taken into account for the forest land use classes. For all three forest land use classes, i.e. mixed forest, deciduous forest and coniferous forest, the German average tree height of the specific tree class, is defined as the displacement height, and ensures a reduction of the aerodynamic resistance over forests compared to, for example, that over grass land.

In order to investigate the sensitivity to tree height, deposition flux calculations were carried out during which the overall tree height was reduced with 5m, i.e. with 25-30%. The resulting comparison with the standard model run, shows that the effect of such a reduction of tree height is strongly limited, and causes only a 2-3% reduction in the annual total deposition over forested areas (Table 3.6 – Tree height).

Table 3.6 Average deposition fluxes over Germany for the three sensitivity simulations

Species	**Basis**	**Emissions_2004**	**Z_0**	**Tree height**
SO_x	214	245	225	213
NO_y	260	284	282	259
NH_x	511	540	550	507